CAPITAL UNIVERSITY OF SCIENCE AND TECHNOLOGY, ISLAMABAD

MHD Mixed Convection Nanofluid Flow and Heat Transfer in a Cavity with Circular Cylinder

by

Adnan Ahmed

A thesis submitted in partial fulfillment for the degree of Master of philosophy

in the

Faculty of Computing
Department of Mathematics

2019

I dedicated this sincere effort to my lovable **Parents** and elegant **Teachers** whose devotions and contributions to my life are really worthless and whose deep consideration on the part of my academic career, made me consolidate and inspired me as I am upto this grade now.

CERTIFICATE OF APPROVAL

MHD Mixed Convection Nanofluid Flow and Heat Transfer in a Cavity with Circular Cylinder

by

Adnan Ahmed

(MMT163013)

THESIS EXAMINING COMMITTEE

S. No.	Examiner	Name	Organization
(a)	External Examiner	Dr. Mudassar Razzaq	LUMS, Lahore
(b)	Internal Examiner	Dr. Muhammad Afzal	CUST,Islamabad
(c)	Supervisor	Dr. Shafqat Hussain	CUST, Islamabad

Thesis Supervisor
Dr. Shafqat Hussain
October, 2019

Dr. Muhammad Sagheer
Head
Dept. of Mathematics
October, 2019

Dr. Muhammad Abdul Qadir
Dean
Faculty of Computing
October, 2019

Author's Declaration

I, **Adnan Ahmed** hereby state that my M.Phil thesis titled "**MHD Mixed Convection Nanofluid Flow and Heat Transfer in a Cavity with Circular Cylinder**" is my own work and has not been submitted previously by me for taking any degree from Capital University of Science and Technology, Islamabad or anywhere else in the country/abroad.

At any time if my statement is found to be incorrect even after my graduation, the University has the right to withdraw my M.Phil Degree.

(Adnan Ahmed)

(MMT163013)

Plagiarism Undertaking

I solemnly declare that research work presented in this thesis titled "**MHD Mixed Convection Nanofluid Flow and Heat Transfer in a Cavity with Circular Cylinder**" is solely my research work with no significant contribution from any other person. Small contribution/help wherever taken has been dully acknowledged and that complete thesis has been written by me.

I understand the zero tolerance policy of the HEC and Capital University of Science and Technology towards plagiarism. Therefore, I as an author of the above titled thesis declare that no portion of my thesis has been plagiarized and any material used as reference is properly referred/cited.

I undertake that if I am found guilty of any formal plagiarism in the above titled thesis even after award of M.Phil Degree, the University reserves the right to withdraw/revoke my M.Phil degree and that HEC and the University have the right to publish my name on the HEC/University website on which names of students are placed who submitted plagiarized work.

(Adnan Ahmed)

(MMT163013)

Acknowledgements

All the praises to Almighty **Allah** the creature of universe and all creators in the universe, who has created us as a human the best creature of the universe. Many thanks to him who created us as a muslim and bless us with the Holy Prophet, **Hazrat Muhammad (sallallahu Alaihay wa'alihi wassalam)** for whom the whole universe is created, who **(Sallallahu Alaihay wa'alihi wassalam)** tell us the difference between right and wrong. I express my heart-felt gratitude to my supervisor **Dr. Shafqat Hussain** for his passionate interest, superb guidance and inexhaustible inspiration through out this work. I would like to acknowledge **CUST** for providing me such a favorable environment to conduct this research. May Almighty Allah shower His choicest blessings and prosperity on all those who helped me in any way during the completion of my thesis.

(Adnan Ahmed)

(MMT163013)

Abstract

Two dimensional, laminar and steady mixed convective flow in a square cavity is studied numerically by using finite element technique. The working fluid is considered as copper-water nanofluid. The circular body with constant radius is placed in the cavity, vertical surfaces of the cavity are taken adiabatic, the upper surface is maintained at cold temperature and moving at a constant speed and lower wall is maintained at hot temperature. The governing equations are discretized using pair bi-quadratic element and discontinuous linear element , the discretized system of non-linear equations are linearized using Picard iteration method, respective linear subproblems are solved using Gaussian elimination method. Final results are shown using isotherms and streamlines.

Contents

List of Figures

List of Tables

Abbreviations

b/w	Between
FEM	Finite Element Method
GFEM	Galerkin Finite Element Method
PDEs	Partial Differential Equations

Symbols

g	Gravitational Acceleration
G_r	Grashof Number
H	Cavity Side Length
Nu	Nusselt Number
P	Dimensionless Fluid Pressure
Pr	Prandtl Number
Re	Reynolds Number
Ri	Richardson Number
r_0	Radius of the Cylinder
r_0/H	Non-Dimensional Radius of the Cylinder
T	Temperature
t	Time
u	Velocity in x-Direction
u_0	Lid Speed
U	Dimensionless Horizontal Velocity
v	Velocity in y-Direction
V	Dimensionless Vertical Velocity
x, y	Cartesian Coordinates
X, Y	Dimensionless Cartesian Coordinates
Greek Symbols	
α	Thermal Diffusivity of the Fluid
β	Coefficient of Thermal Expansion of Fluid
ν	Kinematic Viscosity

θ	Dimensionless Temperature
ρ	Density
ψ	Dimensionless Stream Function
	Subscripts
h	Hot
nf	Nanofluids
f	Base Fluids
s	Nano Size Particles

Chapter 1

Introduction

Heat transfer is a phenomenon in which some amount of heat transfers from high to low temperature region. It occurs when a body has different temperature with respect to its surrounding to equate body temperature with its surrounding. Fluid flows and heat transport in a lid driven square enclosures have many applications in heat exchangers, microelectronic cooling devices, heating and ventilation system in building, solar energy converters, and food heating and cooling devices [1]. Effect of different obstacles on combined convective flow and characteristic of heat transport in a lid driven enclosure with one heated wall attained the focus of many researchers. Paramane and Sharma [2] investigated the heat flow within circular rotating cylinder kept at constant temperature in a 2D lid driven regime and concluded that the average Nusselt number is increased with enhancing Reynolds number. Sivasankaran *et al.* [3] analyzed the impact of different Ricahrdson numbers and the impact of movement of walls in different directions on heat flow in a lid driven square enclosure. They concluded that flow and temperature both are effected due to direction of moving wall. It was also concluded that the heat transport is more prominent at lower values of Ricahrdson number. The flows in lid driven square enclosures with one hot wall have gained the extra attention from researchers. Moreover, the flows in a lid driven square enclosures with one hot and one moving wall also received great attention by recent studies. Omari [4] explored the combined convective flow and heat transport in lid driven enclosure

with one hot wall. He found enhancement in the local Nusselt number by diminishing aspect ratio for $Re = 100$. Mansour *et al.* [5] numerically simulated the steady state three dimensional mixed convective flow and characteristics of heat transport for different values of Ri in square lid driven enclosure. They found that the rate of heat transfer grows due to enhancement in Ri. Basak *et al.* [6] examined the mixed convective flow inside a square enclosure with one cold wall, fixed lower wall, and the upper moving insulated wall by using FEM. They noted for fixed Grashof and Prandtl numbers and by increasing Re the effect of forced convection increased and the effects of the natural convection decreased.

The combination of forced convection and natural convection is called mixed convection. In natural convection fluid motion occur due to natural means, i.e., buoyancy effects due to temperature differences and in forced convection it is due to external forces. If motion of fluid generated due to external source is called forced convection and if the fluid motion not generated due to external source is called natural convection. In the past few years, a huge amount of work has been focused to analyze the impact of blockade on mixed convective flow in different types of cavities with various boundaries. Effect of circular cylinder on mixed convection flows for distinct boundary conditions in a lid driven square cavities have received extraordinary attention of researchers due to its practical applications in different fields like nuclear reactor [7] solar power [8] etc. Cesini *et al.* [9] numerically studied the natural convection inside a rectangular cavity along with horizontal cylinder and investigated the impact of Rayleigh number on heat transfer. Yahiaoui *et al.* [10] analyzed the combined convective flow, and heat transfer due to rotating circular and isothermal cylinder placed inside a horizontal channel. They found that for the fixed rotation rate, by increasing Richardson and Reynolds numbers the average Nusselt number was increased. Raimundo and Costa [11] examined the combined convection in differentially heated square cavity with a circular rotating blockage and found that for the large cylinder radius the Nusselt number was decreased and for low rotating velocity it was increased.

Khanafer and Aithal [12] have investigated the combined convection heat transfer with circular rotating cylinder in lid-driven enclosure and observed that the rate of heat transfer was maximum by placing the rotating cylinder as compared with non-rotating cylinder inside the cavity. Raji and Hasnaoui [13] simulated the combined convection heat transfer rate in ventilated cavity. They examined the flow fields, heat transfer and temperature field for distinct Reynolds and Rayleigh numbers. Ferdousi [14] examined the effect of different Prandtl numbers on the mass transfer and mixed convection with heated circular obstacle in a triangular enclosure. Finally, it was concluded that at high Prandtl number heat transport rate increased rapidly and at low Prandtl number it was increased linearly by the increase of Richardson number. Mansour *et al.* [5] studied the three dimensional mixed convectional flow for fixed Re and for different Ri in lid driven cubic cavity heated from below and solved the dimensionless system of governing equations using the finite element method (FEM). The flow field and characteristics of heat transfer have been examined by means of average Nusselt number, isotherms and streamlines. Saha and Ali [15] numerically inspected the influence of ventilated rectangular enclosure on combined convection for various Re and Ri. It was concluded that by enhancing the value of Re leads to high heat transfer coefficient. Roslan *et al.* [16] numerically analyzed the impact of presence of heated polygon on the free convection and heat transport in square enclosure. Increase in the heat transfer rate has been recorded by enlarging the size of solid polygon. Rehman *et al.* [17] analyzed numerically the impact of different cylinder locations on the combined convection, heat transfer in square enclosure for different Ri using FEM. They observed that different locations of the cylinder had beneficial impact on the flow and thermal fields. Ghasemi and Aminossadati [18] investigated the impact of different Rayleigh numbers on the combined convection in a rectangular cavity. They noted maximum surface temperature of the heat sources for large Rayleigh number.

Nanofluid is the combination of nano-sized particles and the base fluid [19]. Engine

oil and water are commonly considered base fluids and copper, aluminum and silver are some examples of nanoparticles. Nanofluid has improved thermo-physical properties as compared with its corresponding base fluid. Nanofluid has numerous applications in solar water heating, engine cooling, transformer oil cooling, cooling of heat exchanging equipments, cooling of electronics, domestic freezers and refrigerator etc. The thermal properties of nanofluids are significantly better than of corresponding base fluid.

Magneto-hydrodynamics (MHD) deals with magnetic behavior and properties of electrically conducting fluid. MHD has gained the attention of investigators due to its numerous applications in engineering like crystal growth, the fluid flow in microelectronic devices, and the flow of liquid metals [20]. Garmroodi *et al.* [20] simulated numerically the MHD combined convective flow in lid driven enclosure with two rotating cylinders inside it. They conclude that by enhancing the Hartmann number heat transfer rate is reduced. Kabir *et al.* [21] investigated the impact of viscous dissipation on magnetohydrodynamics natural convectional flow with a vertical wavy surface. They concluded that the velocity and temperature increases by increasing the Eckert number. Uddin *et al.* [22] examined the influence of mass transfer rate on MHD mixed convection along with inclined porous plate. They concluded that by increasing Grashof number the temperature decreases and heat transfer rate increases. Fateh and Oudina [23] numerically analyzed the hydrodynamics and thermal characteristics of nanofluids filled in a cylindrical cavity. It was analyzed that the heat transport increases by increasing the Rayleigh number and with nanoparticles volume fraction. Gul *et al.* [24] studied the heat transfer in MHD combined convective flow of ferrofluids in a vertical channel. They concluded that by increasing volume fraction, the thermal conductivity and the nanofluids viscosity increased. Veeresh *et al.* [25] analyzed the mass and heat transport in MHD combined convective flow on moving inclined porous plate. They observed that by enhancing the heat source parameter caused in decrease of temperature distribution.

1.1 Thesis Contribution

In the present work we will focus on the impact of circular cylinder and various governing parameters on the combined convective nanofluid flow and characteristics of heat transport in a square lid driven enclosure. The nondimensional form of the governing partial differential equations are discretized and solved by using the higher order FEM. By means of plots, streamlines, and isotherms the effect of controlling parameters on the flow field and heat transport will be discussed in the presence of circular blockade in the lid driven enclosure. Adiabatic boundary condition that is imposed and examined on the circular body.

1.2 Thesis Outline

This study is further divided into the following four chapters:

Chapter 2 contains the basic definitions, laws and terminologies related to heat transfer and fluid flow, which are important to understand the work presented in the upcoming chapters. Basic philosophy of the FEM is also discussed in this chapter.

Chapter 3 contains the review study of the work presented in [26]. In this chapter the laminar, steady and incompressible combined convective flow and characteristics of heat transport in the presence of circular body inside a square lid driven enclosure is numerically analyzed. The biquadratic Q_2 element is used to discretize the velocity and temperature components, and for pressure components discontinuous linear P_1^{disc} is used. In the form of isotherms and streamlines the impact of various boundary condition imposed on cylinder, and Ri on flow and

heat transport have been compared.

Chapter 4 extends the work of Khanafer [26] by adding copper nanoparticles in the base fluid. The governing equations have been dealt in same manner as aforementioned in Chapter 3.

Chapter 5 consists of the conclusion of the entire thesis.

Chapter 2

Fundamental Terminologies and Laws of Fluid Dynamics

This chapter contains some important laws, terminologies and definitions which are important and essential to understand the work presented in the next chapters.

2.1 Important Definitions

There are some important definitions and concepts related to the work presented in the next chapters. [27]

Definition 2.1. Fluid [28]

"Fluids are substances whose molecular structure offers no resistance to external shear forces: even the smallest force causes deformation of a fluid particle. Although a significant distinction exists between liquids and gases, both types of fluids obey the same laws of motion."

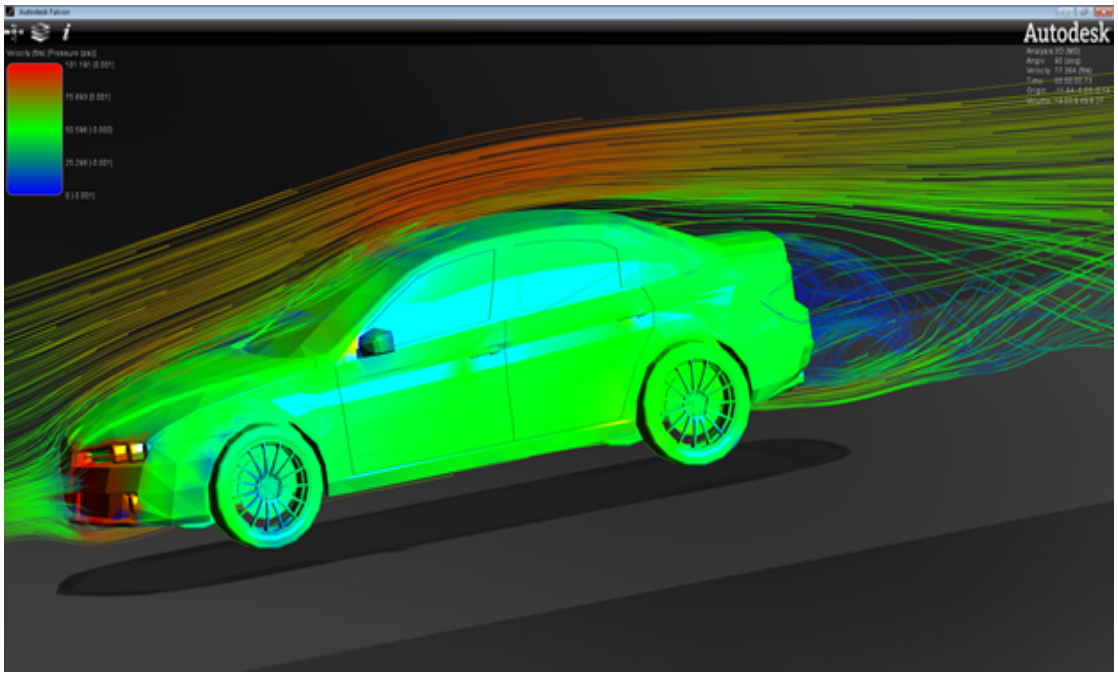

Definition 2.2. Fluid Mechanics [29]

"Fluid mechanics is that branch of science which deals with the behavior of the fluids (liquids or gases) at rest as well as in motion. Thus this branch of science deals with the static, kinematics and dynamic aspects of fluids."

Definition 2.3. Fluid Statics [29]

"The study of fluids at rest is called fluid statics.Fluid statics is generally referred to as hydrostatics when the fluid is a liquid and as aerostatics when the fluid is a gas.

Newton's second law for non-accelerating bodies is used to describe the basic equation of fluid statics,"

$$\sum F = 0.$$

Definition 2.4. Fluid Kinematics [29]

"The study of the fluids in motion, where pressure forces are not considered, is called fluid kinematics."

Definition 2.5. Fluid Dynamics [29]

"If the pressure forces are also considered for the fluids in motion, that branch of science is called fluid dynamics.

Newton's second law of motion for accelerating bodies is used to represent the equation of fluid dynamics,"

$$\sum F = ma.$$

Definition 2.6. **Viscosity**

"Viscosity is defined as the property of a fluid which offers resistance to the movement of one layer of fluid over another adjacent layer of the fluid."

Definition 2.7. **Dynamic Viscosity**

"The extent which measures the resistance of fluid tending to cause the fluid to flow is called dynamic viscosity, also known as absolute viscosity. This resistance arises from the attractive forces between the molecules of the fluid. Usually liquids and gasses have non-zero viscosity. It is denoted by symbol μ and mathematically, it can be written as,

$$\mu = \frac{shearstress}{shearstrain},$$

here μ is called the coefficient of viscosity. Unit of viscosity in SI system is $\frac{kg}{ms}$ or Pascal-second."

Definition 2.8. **Kinematic Viscosity**

"It is the ratio between the dynamic viscosity and density of fluid, and mathematically it can be written as

$$\nu = \frac{\mu}{\rho}."$$

Definition 2.9. **Nanofluids**

"Nanofluids are engineered colloids made of a base fluid and nanoparticles (1-100)nm. Nanofluids have higher thermal conductivity and single-phase heat transfer coefficients than their base fluids Metals, oxides, carbides, or carbon nanotubes are the typical nanoparticles which are used in nanofluids and oil, ethylene glycol and water are the examples of common base fluids."

2.2 Stress and its Types

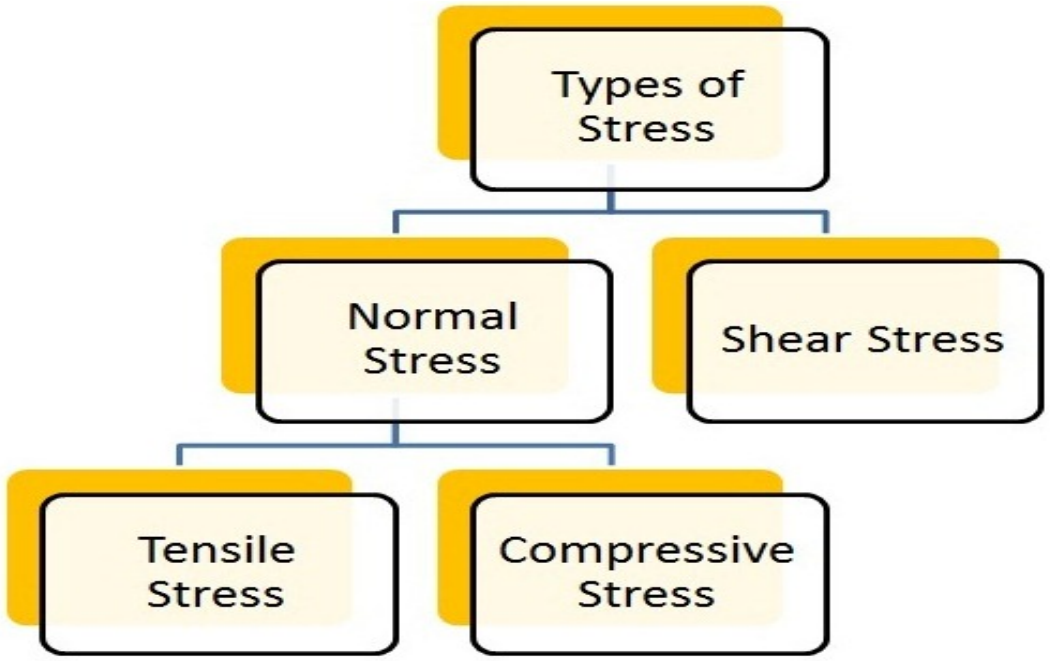

Definition 2.10. Stress

"Stress is a force which acts parallel or perpendicular to the material surface per unit its area and is denoted by σ It is a tensor quantity". Mathematically, it can be written as;

$$\sigma = \frac{F}{A}$$

where F represents force and A denotes area.

Definition 2.11. Shear Stress

"It is a type of stress in which force vector acts parallel to the material surface or cross section of a material."

Definition 2.12. Normal Stress

"Normal stress is a type of stress in which force vector acts perpendicular to the surface of the material or cross section of a material."

Definition 2.13. Yield Stress

"The property of material at which a matter begins to deform physically until the force acting on it and will back to its original form when the applied force is released."

2.3 Types of Fluids [29]

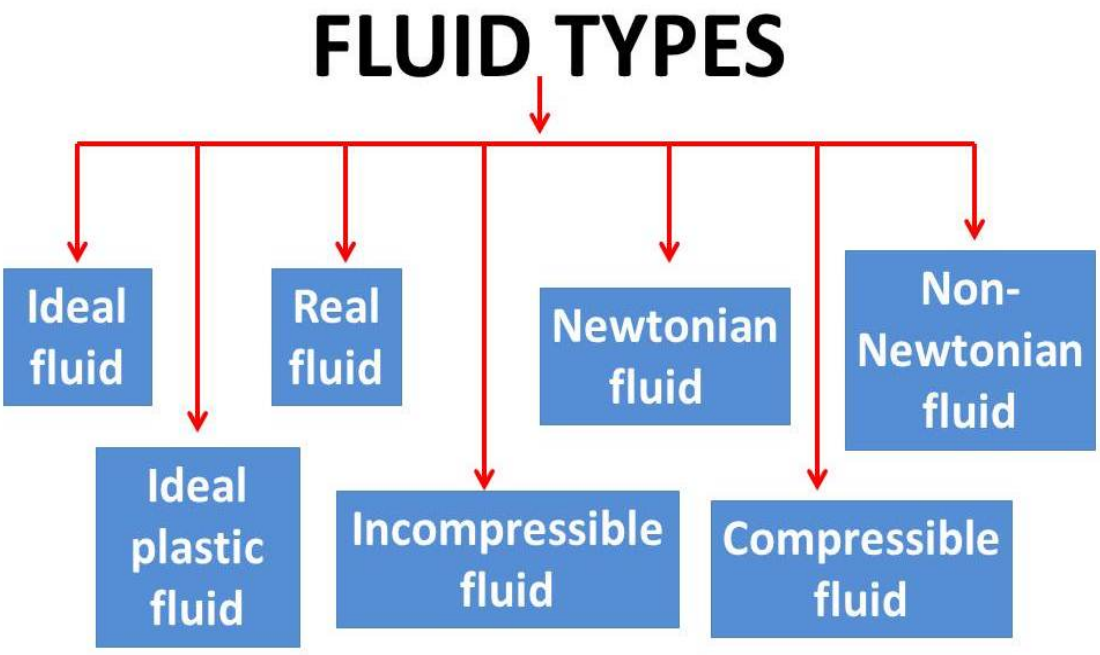

"The fluids may be classified into following five types."

Ideal Fluid

"A fluid, which is incompressible and is having no viscosity, is known as an ideal fluid."

Real Fluid

" A fluid, which possesses viscosity, is known as real fluid. All the fluids,in actual practice, are real fluids."

Ideal Plastic Fluid

" A fluid, in which shear stress is more than the yield value and shear stress is proportional to the rate of shear strain (or velocity gradient), is known as ideal plastic fluid."

Non-Newtonian Fluid

"A real fluid, in which the shear stress is not directly proportional to the rate of

shear strain (or velocity gradient), is known as a non-Newtonian fluid."

Newtonian Fluid

"A real fluid, in which the shear stress is directly proportional to the rate of shear strain (or velocity gradient), is known as a Newtonian fluid."

2.4 Classification of Fluid Flow

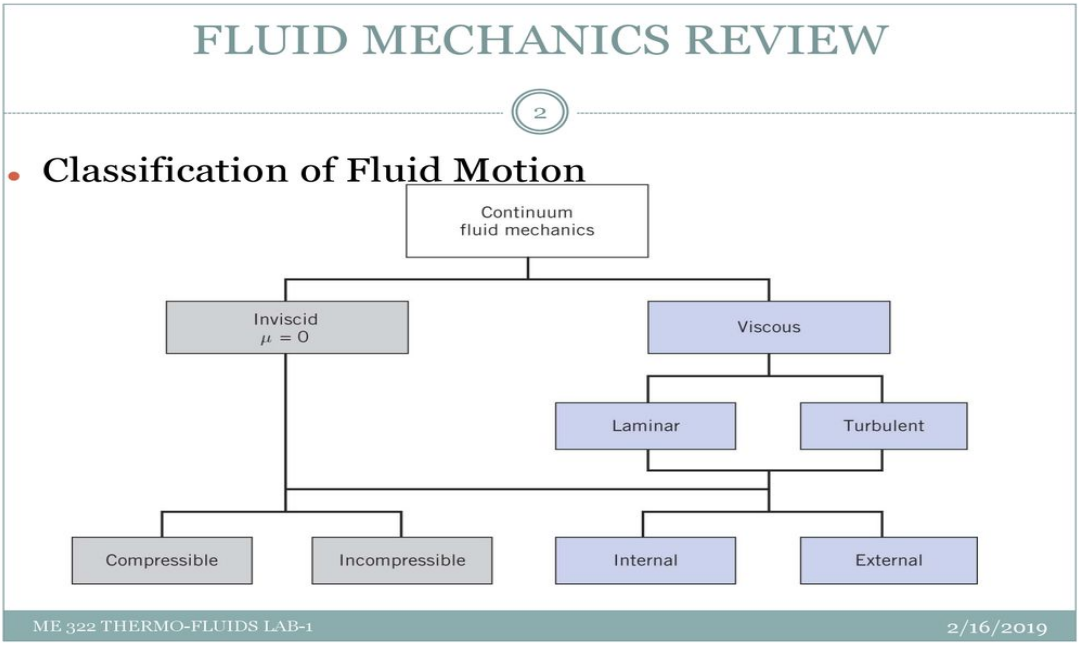

Definition 2.14. Viscous Fluid [30]

"Viscosity is the measure of the internal friction of a fluid. This friction become apparent when a layer of fluid is made to move in relation to another layer. The greater the friction, the greater the amount of force required to cause this movement, which is called shear."

Definition 2.15. Internal and External Flow [31]

"The flow of an unbounded fluid over a surface such as a plate, a wire, or a pipe is external flow. The flow in a pipe or duct is internal flow if the fluid is completely bounded by solid surfaces."

Definition 2.16. Laminar and Turbulent Flows [28]

"Fluid particle follows a smooth trajectory; the flow is then said to be laminar. Further increases in speed may lead to instability that eventually produces a more random type of flow that is called turbulent."

Definition 2.17. Compressible and Incompressible Flows [31]

"A fluid flow during which the density of the fluid remains nearly constant is called incompressible flow. A fluid whose density is practically independent of pressure (such as a liquid) is called an incompressible fluid. The flow of compressible fluid (such as air) is not necessarily compressible since the density of a compressible fluid may still remain constant during flow."

Definition 2.18. Steady and Unsteady Flow [31]

"A process is said to be steady-flow if it involves no changes with time anywhere within the system or at the system boundaries and a process is said to be unsteady-flow if it changes with time anywhere within the system or at the system boundaries."

Definition 2.19. Natural and Force Flow [31]

"In forced flow, the fluid is forced to flow over a surface or in a tube by external means such as a pump or a fan. In natural flow, any fluid motion is caused by natural means such as the buoyancy effect that manifests itself as the rise of the warmer fluid and the fall of the cooler fluid. The flow caused by winds is natural flow for the earth, but it is forced flow for bodies subjected to the winds since for the body it makes no difference whether the air motion is caused by a fan or by the winds."

Definition 2.20. Uniform and Non-Uniform Flow

"Uniform flow is defined as, a flow in which the velocity at any given time does not change with respect to space(i.e., length or direction of the flow)." Mathematically

$$\left(\frac{\partial \mathbf{V}}{\partial s}\right)_{t=constant} = 0$$

"Non-uniform flow is that type of flow in which the velocity at any given time change with respect to space." Mathematically

$$\left(\frac{\partial \mathbf{V}}{\partial s}\right)_{t=constant} \neq 0$$

2.5 Heat Transfer Mechanism and Properties

2.6 Classification of Fluid Flow

Definition 2.21. **convection**

" Convection, relates to the transfer of heat from a bounding surface to a fluid in motion, or to the heat transfer across a flow plane within the interior of the flowing fluid." Mathematically

$$\dot{Q} = hAT_s - T_\infty.$$

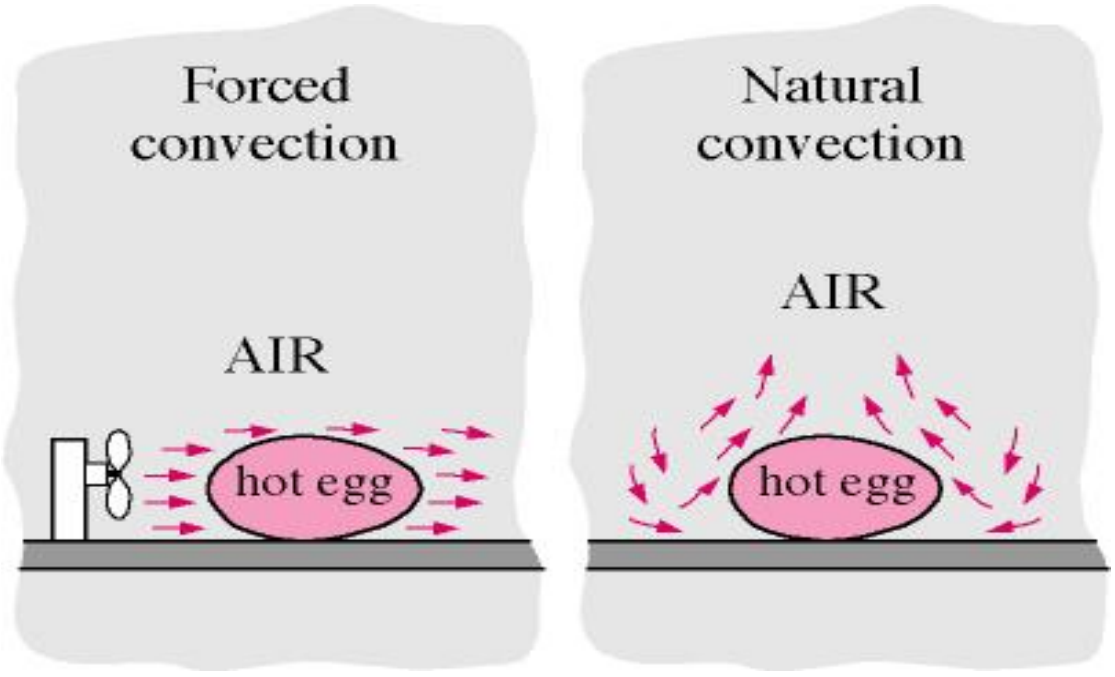

Definition 2.22. **Natural Convection** [32]

"When fluid motion occurs because of a density variation caused by temperature differences, the situation is said to be a free, or natural, convection."

Definition 2.23. Forced Convection [32]

"When fluid motion is caused by external force, such as pumping or blowing, the state is defined as being one of forced convection."

Definition 2.24. Mixed Convection [32]

"Mixed convection involves features from both Forced convection and Natural convection.

For example if fluid is moving vertically upward along the moment of the vertical stretching sheet is forced convection while in the same phenomena fluid is freely falling due to the gravity which is free convection. When these two phenomena appear in the same model then such kind of flow is mixed convection."

Definition 2.25. Heat

"In thermodynamics heat is defined as the form of energy that is transferred across the boundary of a system at a given temperature to another system(or the surroundings) at a lower temperature by virtue of the temperature difference between the two systems."

Definition 2.26. Heat Transfer [32]

" Heat transfer is that section of engineering science that studies the energy transport between material bodies due to a temperature difference."

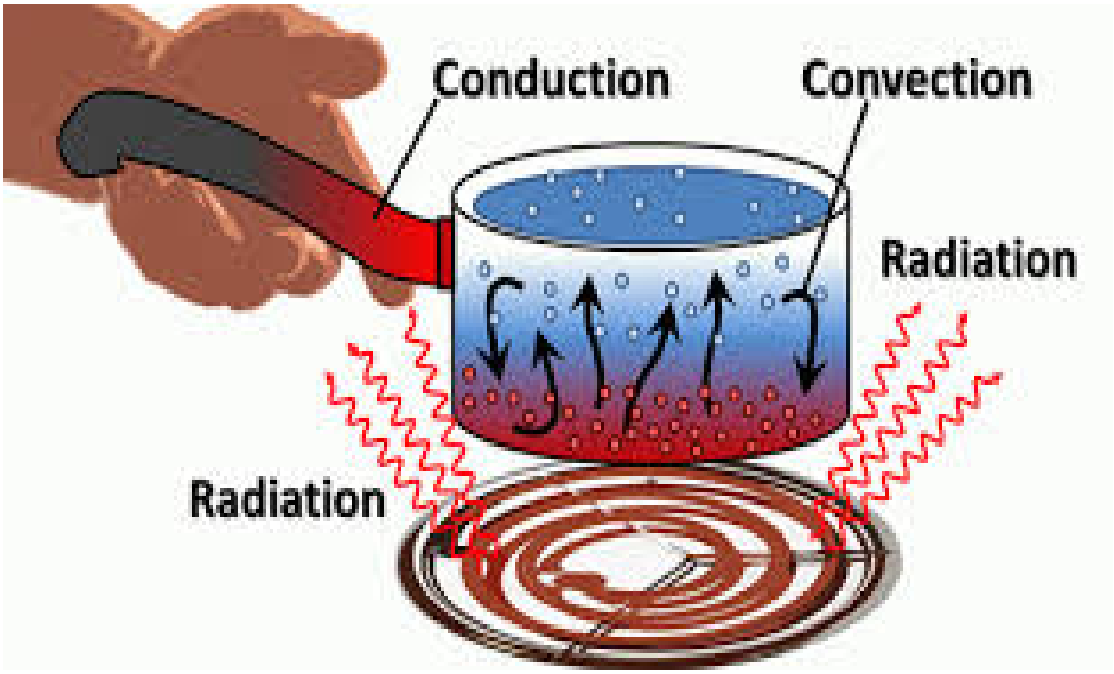

Definition 2.27. Modes of Heat Transfer [32]

"There are three modes of heat transfer conduction, convection and radiation."

Definition 2.28. Conduction [32]

"The conduction mode of heat transfer occurs either because of an exchange of energy from one molecule to another, without the actual motion of the molecules, or because of the motion of the free electrons of they are present. This form of heat transfer occurs in solids, liquids and gases."

Definition 2.29. Convection [32]

"Molecules present in liquids and gases have freedom of motion, and by moving from hot to cold region, they carry energy with them. The transfer of heat from one region to another , due to such macroscopic motion in a liquid and gas, added to the energy transfer by conduction within the fluid, is called heat transfer by convection."

Definition 2.30. Radiation [32]

"All bodies emit thermal radiation at all temperature. This is the only mode in which both does not require a material medium for heat transfer to occur. The nature of thermal radiation is such that a propagation of energy, carried by electromagnetic waves, is emitted from the surface of the body. When these electromagnetic waves strike other body surface, a part is reflected, a pert is transmitted and the remaining part absorbed."

2.7 Some Impotant Definitions

Definition 2.31. Streamlines [33]

"A streamline is a line everywhere tangent to the velocity field. For two-dimensional flows the slop of the streamline must be equal to the tangent of the angle that the velocity angle makes with the x-axis."

Definition 2.32. Stream function [32, 33]

"Stream function is a very useful device in the study of fluid dynamics. Stream

function is often used to draw the streamlines in order to better understand the flow pattern around a body. A stream function ψ is one which satisfies $u = \frac{\partial \psi}{\partial y}$, $v = u = \frac{\partial \psi}{\partial x}$."

Definition 2.33. Isothermal Process [29] "If the change in density occurs at constant temperature, then the process is called isothermal and relationship between pressure (p) and density (ρ) is given by
$\frac{p}{\rho}$=Constant."

Definition 2.34. Adiabatic Process [29] "If the change in density occurs with no heat exchange to and from the gas, the process is called adiabatic. And if no heat is generated within the gas due to friction, the relationship between pressure and density is given by
$\frac{p}{\rho^k}$=Constant
where k=Ratio of the specific heat of a gas at constant pressure and constant volume."

Definition 2.35. Viscous Dissipation [28]
"Viscous dissipation represents the irreversible (in the thermodynamic sense) conversion of kinetic energy of the flow into internal energy of the fluid".

Definition 2.36. Thermal Conductivity [34]
"Thermal conductivity k is a measure of the ability of a material to conduct heat. Mathematically

$$k = \frac{q \nabla l}{S \nabla T}$$

where q is the heat passing through a surface area S and the effect of a temperature difference ∇T over a distance is ∇l. Here l, S and ∇T all are assumed to be of unit measurement."

Definition 2.37. Joule Heating "Joule heating is the energy dissipation that occurs with an electric current flowing through a resistor."

Definition 2.38. Thermal Diffusivity
"It measures the ability of material to conduct thermal energy relative to its ability

to store thermal energy means how fast or how easily heat can penetrate an object or substance. Mathematically

$$\alpha = \frac{k}{\rho C_p},$$

Where k is the thermal conductivity ρ is the density and C_p is the specific heat."

Definition 2.39. Density

"Concentration of mass per unit volume is termed as density of material. Symbolically, it is represented by greek letter ρ and mathematically written as

$$\rho = \frac{m}{V},$$

here V and m are the volume and mass of the material."

Definition 2.40. Pressure

"The component of applied force perpendicular to the surface of an object per unit area is termed as pressure. It is represented by P and mathematically, it is written as

$$P = \frac{F}{A},$$

where F and A denote the applied force and area of the surface."

Definition 2.41. Newton's Law of Viscosity

"It states that the shear stress is proportional to the deformation rate of the fluid. Mathematically it is written as

$$\tau_{yx} = \mu \frac{du}{dy},$$

where the symbol τ_{yx} is the shear stress, x and y represents horizontal and vertical coordinates, u is the horizontal component of velocity, μ is the constant of proportionality termed as dynamic viscosity while $du\ dy$ is the deformation rate."

Definition 2.42. Boundary Layer

"Boundary layer is a flow layer of fluid close to the solid region of the wall in contact where the viscosity effects are significant. The flow in this layer is usually

laminar. The boundary layer thickness is the measure of the distance apart from the surface."

Definition 2.43. specific Heat

"The specific heat is that amount of heat which is necessarily added to increase one unit temperature of one unit area."

Definition 2.44. Magnetohydrodynamics(MHD) [35]

"Magnetohydrodynamics (MHD) is concerned with the flow of electrically conducting fluids in the presence of magnetic fields, either externally applied or generated within the fluid by inductive action."

2.8 Laws of Conservation and Basic Equations

"There are three laws of conservation which are used to model the problems of fluid dynamics, and may be written in integral or differential form. Integral formulations of these laws consider the change of mass, momentum or energy within the control volume" [36].

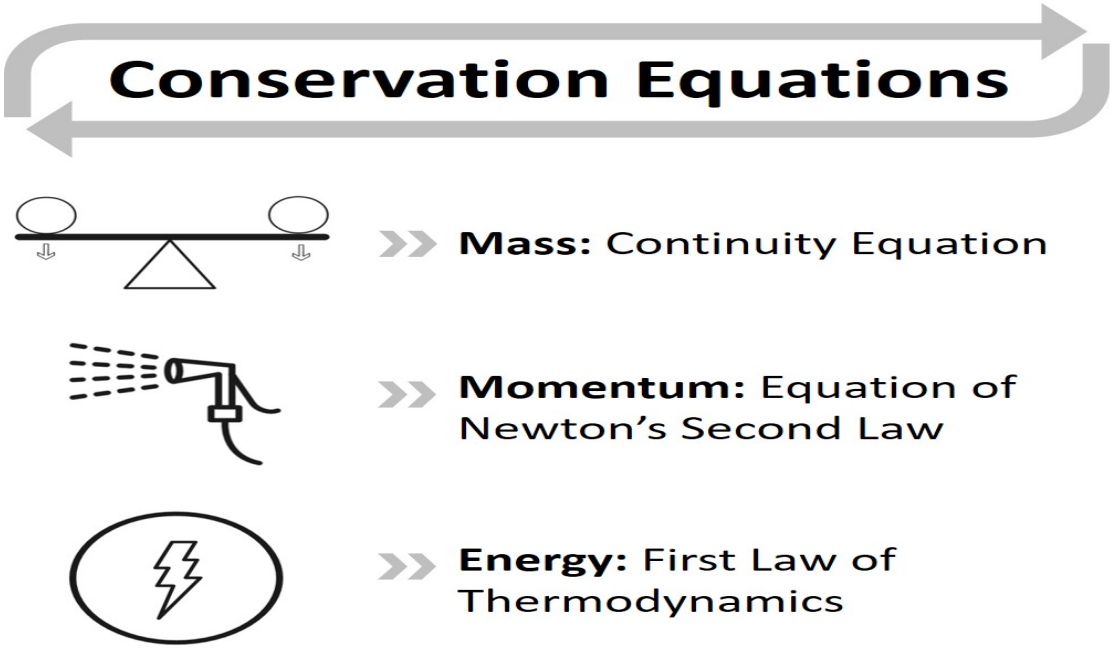

2.8.1 Continuity Equation [36]

"The conservation of mass of fluid entering and leaving the control volume, the resulting mass balance is called the equation of continuity." This equation reflects the fact that mass is conserved. For any fluid, conservation of mass is expressed by the scaler equation

$$\frac{\partial \rho}{\partial t} + \nabla.[(\rho)\mathbf{V}] = 0,$$

$$\Longrightarrow$$

$$\frac{\partial \rho}{\partial t} + \nabla.(\rho\mathbf{V}) = 0. \tag{2.1}$$

Hence, a velocity profile represents a real flow, if and only if it satisfies the continuity equation. For incompressible fluids, Eq. (2.1) reduces to

$$\nabla.\mathbf{V} = 0."$$

2.8.2 Momentum Equation[34, 36]

"The product of the mass and the velocity of a body is called the linear momentum. Newton's second law states that the acceleration of a body is proportional to the net force acting on it and is inversely proportional to its mass, and that the rate of change of the momentum of a body is equal to the net force acting on the body. Therefore, the momentum of a system remains constant when the net force acting on it is zero, and thus the momentum of such systems is conserved. This is known as the conservation of momentum principle.

For any fluid, the momentum equation is

$$\frac{\partial(\rho\mathbf{V})}{\partial t} + \nabla.[(\rho\mathbf{V})\mathbf{V}] - \nabla.(\mathbf{T}) - (\rho\mathbf{g}) = 0. \tag{2.2}$$

Since $\mathbf{T} = -p\mathbf{I} + \tau$, the momentum equation takes the form

$$\rho\left(\frac{\partial \mathbf{V}}{\partial t} + \mathbf{V}.\nabla\mathbf{V}\right) = \nabla.(-p\mathbf{I} + \tau) + \rho\mathbf{g}. \tag{2.3}$$

Eq. (2.3) is a vector equation and can be decomposed further into three scalar components by taking the scalar product with the basis vectors of an appropriate orthogonal coordinate system. By setting $\mathbf{g} = -g\nabla z$, where z is the distance from an arbitrary reference elevation in the direction of gravity, Eq. (2.3) can be also expressed as

$$\rho\left(\frac{\partial \mathbf{V}}{\partial t} + \mathbf{V}.\nabla\mathbf{V}\right) = \nabla.(-p\mathbf{I} + \tau) + \nabla(-\rho g z). \tag{2.4}$$

The momentum equation then states that the acceleration of a particle following the motion is the result of a net force, expressed by the gradient of pressure, viscous and gravity forces".

2.8.3 Energy Equation [34]

"One of the most fundamental laws in nature is the first law of thermodynamics, also known as the conservation of energy principle. It states that energy can be neither created nor destroyed during a process; it can only change forms". Energy equation in vector form for base fluid can be expressed as

$$\mathbf{v}.\nabla T = \alpha\nabla^2 T.$$

2.9 Dimensionless Numbers

Dimensionless numbers have important role in fluid mechanics. Some dimensionless numbers are defined below.

Definition 2.45. **Nusselt Number (N_u)** [37]

" It expresses the ratio of the total heat transfer in a system to the heat transfer by conduction. It characterizes the heat transfer by convection between a fluid and the environment close to it or, alternatively, the connection between the heat transfer

intensity and the temperature field in a flow boundary layer," Mathematically

$$\text{“}N_u = \frac{\alpha H}{\lambda},$$

where H is the characteristic length, α is the heat transfer coefficient, and λ is thermal conductivity".

Definition 2.46. Grashof Number (Gr) [37]

"It express the buoyancy to viscous forces ratio and its action on fluid. It characterizes the free non-isothermal convection of the fluid due to the density difference caused by the temperature gradient in the fluid, Mathematically

$$Gr = \frac{H^3 g\beta \triangle T}{\nu^2},$$

where g is acceleration due to Earth's gravity, H is the characteristic length, g is gravitational acceleration, $\triangle T$ is temperature change, ν is the kinematic viscosity, β coefficient of thermal expansion of fluid."

Definition 2.47. Reynolds Number (Re) [37]

"This number expresses the ratio of the fluid inertia force to that of molecular friction (viscosity). It determines the character of the flow (laminar, turbulent and transient flows)." Mathematically it can be written as

$$\text{“}Re = \frac{u_0 H}{\nu},$$

where H is characteristic length, u_0 the flow velocity, and ν is density".

Definition 2.48. Prandtl Number (Pr) [37]

"This number expresses the ratio of the momentum diffusivity (viscosity) to the thermal diffusivity. Mathematically it can be written as

$$Pr = \frac{\nu}{\alpha},$$

where ν represents the kinematic viscosity and α denotes thermal diffusivity. It characterizes the physical properties of a fluid with convective and diffusive heat transfers."

Definition 2.49. Richardson Number (Ri)

"Richardson number is a non-dimensional parameter named after Lwis Fry Richardson (1881-1953). This number expresses the potential-to-kinetic energies ratio.

$$Ri = \frac{g\ H}{u^2}$$

g- gravitational acceleration, H-the cavity length, u the characteristic flow velocity".

Definition 2.50. Hartmann Number (Ha) [37]

"It is an important criterion of magneto-hydrodynamics. It expresses the ratio of the induced electrodynamic (magnetic) force to the hydrodynamic force of the viscosity. It characterizes the magnetic field influence on the flow of viscous, electrically conducting fluid." Mathematically

$$Ha = BH\sqrt{\frac{\gamma}{\eta}}$$

H is the cavity length, B is magnetic induction, and η dynamic viscosity and γ specific electrical conductance."

Definition 2.51. Eckert Number (Ec) [37]

"It expresses the ratio of kinetic energy to a thermal energy change." Mathematically,

$$Ec = \frac{w_\infty^2}{C_p \triangle T},$$

C_p, the specific heat, w_∞^2 velocity of fluid far from body, $\triangle T$ the temperature difference.

2.10 Finite Element Method(FEM) [28]

"The finite element method is similar to the finite volume method in many ways. The domain is broken into a set of discrete finite elements in 2D, they are usually triangles or quadrilaterals, while in 3D tetrahedra or hexahedra are most often used. The equations are multiplied by a weight function before they are integrated over the entire domain. In the simplest finite element methods, the solution is approximated by a linear shape function within each element is a way that guarantees continuity of the solution across element boundaries. Such a function can be constructed from its values at the corners of the elements. The weight function is usually of the same form. This approximation is then substituted into the weighted integral of the conservation law and the equations to be solved are derived by requiring the derivative of the integral with respect to each nodal value to be zero; this corresponds to selecting the best solution within the set of allowed functions (the one with minimum residual). The result is a set of non-linear algebraic equations."

Galerkin Finite Element Method(GFEM)

"In numerical analysis the Galerkin finite element is a method which is used to transform the continuous operator problems (that is differential) into discrete problems. It converts the governing equations from strong to weak form and then used to obtain the approximate solution. This method is given below:

- Let R be the residual of the model problem. Multiply R by a test function $w \in W$, which satisfy the homogeneous Dirichlet boundary conditions.
- Integrate the weighted residual over the whole domain Ω to transfer some derivatives from trail function ($u\ in\ V$) to test function ($w\ in\ W$).
- Apply Neumann or Robin boundary conditions to attain the weak form.

- Approximate $u = u_h \in V_h$ and $w = w_h \in W_h$, where V_h and W_h are finite dimensional trail and test spaces respectively.

- Choose basis $s_1, s_2, s_3, \ldots s_N \in W_h$ such that each test function can be written as a linear combination of these basis functions,

$$w_h = \sum_{i=1}^{N} w_i s_i \quad \in W_h,$$

and approximate solution

$$u_h = \sum_{j=1}^{N} u_j s_j \quad \in V_h,$$

by substituting u_h and w_h in weak form and then by evaluating we get the linear system of the form

$$A\ U = F, \tag{2.5}$$

where A is the stiffness matrix, U is the vector of required unknowns and F is the R.H.S vector. Then solve Eq.(2.5) for N unknowns coefficients $u_j's$".

Example Consider a steady Poisson equation in 2D.

$$-\Delta\ \theta = f \quad in\ \ \Omega, \tag{2.6}$$

$$\theta = 0 \quad in\ \ \partial\Omega \tag{2.7}$$

θ is to be found, f is known, Ω is domain which is bounded, open and connected and $\partial\Omega$ is the boundary.

The exact solution $\theta(x, y)$ of the above problem should be twice differentiable and satisfy Eq.(2.6). Let $\tilde{w}$ be test function which satisfy the homogeneous Dirichlet boundary conditions i.e., $\tilde{w} = 0 \quad$ on $\partial\Omega$.

For the weak form, the weighted residual integral of Eq.(2.6) becomes

$$-\int_{\Omega} \tilde{w}\Delta\ \theta\ \partial\Omega = \int_{\Omega} \tilde{w} f\ \partial\Omega. \tag{2.8}$$

Green's theorem is used to shift a derivate from θ on $\tilde{w}$ and we get

$$-\underbrace{\int_{\Gamma} \tilde{w}\nabla\ \theta\partial\Gamma}_{0} + \int_{\Omega} \nabla\tilde{w}\nabla\ \theta\ \partial\Omega = \int_{\Omega} \tilde{w}f\ \partial\Omega, \tag{2.9}$$

boundary integral vanishes on the boundary and we get

$$\int_{\Omega} \nabla\tilde{w}\nabla\ \theta\ \partial\Omega = \int_{\Omega} \tilde{w}f\ \partial\Omega, \tag{2.10}$$

in Cartesian coordinate system Eq.(2.10) can be written as

$$\int_{\Omega} \left(\frac{\partial\tilde{w}}{\partial x}\frac{\partial\theta}{\partial x} + \frac{\partial\tilde{w}}{\partial y}\frac{\partial\theta}{\partial y}\right)\ \partial\Omega = \int_{\Omega} \tilde{w}f\ \partial\Omega, \tag{2.11}$$

elemental weak form is

$$\int_{\Omega^e} \left(\frac{\partial\tilde{w}}{\partial x}\frac{\partial\theta^e}{\partial x} + \frac{\partial\tilde{w}}{\partial y}\frac{\partial\theta^e}{\partial y}\right)\ \partial\Omega = \int_{\Omega^e} \tilde{w}f\ \partial\Omega, \tag{2.12}$$

approximated solution over an element as

$$\theta^e = \sum_{j=1}^{N} \theta_j^e S_j^e, \tag{2.13}$$

where, S_j^e are basis functions and θ_j^e are the solution values at nodes, using Eq.(2.13) in Eq.(2.12) we obtained

$$\int_{\Omega^e} \left(\sum_{j=1}^{N} \theta_j^e \frac{\partial S_j^e}{\partial x}\right) \frac{\partial\tilde{w}}{\partial x}\ \partial\Omega + \int_{\Omega^e} \left(\sum_{j=1}^{N} \theta_j^e \frac{\partial S_j^e}{\partial x}\right) \frac{\partial\tilde{w}}{\partial y}\ \partial\Omega = \int_{\Omega^e} \tilde{w}f\ \partial\Omega, \tag{2.14}$$

by choosing weight function $\tilde{w}= S_i^e$ to get the elemental system's ith equation

$$\int_{\Omega^e} \left(\sum_{j=1}^{N} \theta_j^e \frac{\partial S_j^e}{\partial x}\right) \frac{\partial S_i^e}{\partial x}\ \partial\Omega + \int_{\Omega^e} \left(\sum_{j=1}^{N} \theta_j^e \frac{\partial S_j^e}{\partial x}\right) \frac{\partial S_i^e}{\partial y}\ \partial\Omega = \int_{\Omega^e} \tilde{w}f\ \partial\Omega, \tag{2.15}$$

or

$$\sum_{j=1}^{N} \int_{\Omega^e} \left[\left(\frac{\partial S_j^e}{\partial x}\frac{\partial S_i^e}{\partial x} + \frac{\partial S_j^e}{\partial x}\frac{\partial S_i^e}{\partial y}\right)\right] \theta_j^e\ \partial\Omega = \int_{\Omega^e} \tilde{w}f\ \partial\Omega, \tag{2.16}$$

$$\left[K^e\right]\left\{\theta^e\right\} = \left\{F^e\right\}, \tag{2.17}$$

where the elemental stiffness matrix

$$\left[K^e\right] = \sum_{j=1}^{N} \int_{\Omega^e} \left(\frac{\partial S_j^e}{\partial x}\frac{\partial S_i^e}{\partial x} + \frac{\partial S_j^e}{\partial x}\frac{\partial S_i^e}{\partial y} \right) \partial\Omega,$$

elemental node vector,

$$\left\{\theta^e\right\} = \theta_j^e,$$

right hand side elemental force vector,

$$\left\{F^e\right\} = \int_{\Omega^e} \tilde{w} f \ \partial\Omega,$$

and the corresponding global system can be write as

$$\left[K\right]\left\{\theta\right\} = \left\{F\right\}. \tag{2.18}$$

Chapter 3

Combined Convective Flow and Heat Transport Characteristics in a Enclosure with Circular Body

In this chapter, the combined convective flow and characteristics of heat transport in the presence of a circular body inside a square lid driven enclosure has been investigated using the FEM based on the Galerkin method. Flow and heat transport have been analyzed through average Nusselt number, isotherms and streamlines for the distinct value of Richardson number. Two types of boundary conditions namely isothermal and adiabatic are imposed and studied on the cylinder. This chapter provides the review study of [26].

3.1 Problem Statement

The physical model under study is represented in Figure 3.1. Two dimensional, steady and incompressible flow is investigated in a square enclosure with side length H and a circular cylinder having radius $r_0/H = 0.2$ placed within the cavity. The upper horizontal surface is moving in the positive x-axis direction with fixed speed u_0. Vertical surfaces of the enclosure are taken adiabatic. Cold temperature

T_c and hot temperature T_h are enforced on the top moving and stationary bottom walls, respectively, except $u = u_0$ at the top wall of the cavity no slip boundary conditions are applied on u and v velocities for each wall and cylinder in the cavity. Two types of thermal conditions namely adiabatic and isothermal are tested on the circular cylinder respectively.

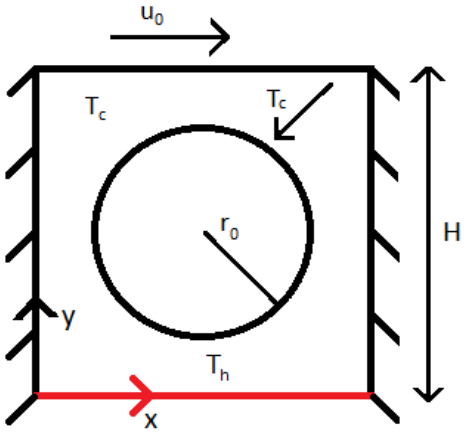

Figure 3.1: Schematic Diagram with Boundary Conditions and Coordinates.

The Governing Equations

Two dimensional system of governing equations consisting of continuity, momentum and energy is [26]

$$\frac{\partial u}{\partial x} + \frac{\partial v}{\partial y} = 0, \tag{3.1}$$

$$u\frac{\partial u}{\partial x} + v\frac{\partial u}{\partial y} = -\frac{1}{\rho}\frac{\partial p}{\partial x} + \frac{\mu}{\rho}\left(\frac{\partial^2 u}{\partial x^2} + \frac{\partial^2 u}{\partial y^2}\right), \tag{3.2}$$

$$u\frac{\partial v}{\partial x} + v\frac{\partial v}{\partial y} = -\frac{1}{\rho}\frac{\partial p}{\partial y} + \frac{\mu}{\rho}\left(\frac{\partial^2 v}{\partial x^2} + \frac{\partial^2 v}{\partial y^2}\right) + (\rho\beta)g(T_h - T_c), \tag{3.3}$$

$$u\frac{\partial T}{\partial x} + v\frac{\partial T}{\partial y} = \alpha\left(\frac{\partial^2 T}{\partial x^2} + \frac{\partial^2 T}{\partial y^2}\right). \tag{3.4}$$

The Dimension Form of the Boundary Conditions

$u = v = 0, \quad T = T_h, \quad \text{at} \quad y = 0, \quad 0 < x < 1,$

$u = u_0, \quad v = 0, \quad T = T_c, \quad \text{at } y = 1, \quad 0 < x < 1,$

$u = v = 0, \quad \frac{dT}{dx}=0, \quad \text{at } x = 0,\ 1, \quad 0 \le y \le 1$

and the boundary conditions for circular cylinder are $u = v = 0$ for the velocity, isothermal and adiabatic are thermal boundary conditions for cylinder.

i.e., T_c or $\frac{\partial T}{\partial \mathbf{n}} = 0$,

where $\mathbf{n}$ is a unit normal vector to the surface to the surface of circular body.

The Dimensionless Governing Equations

We nondimensionalize the governing equations using below dimensionless quantities: $X = \frac{x}{H}$, $Y = \frac{y}{H}$, $U = \frac{u}{u_0}$, $V = \frac{v}{u_0}$, $\theta = \frac{T-T_c}{T_h-T_c}$, $P = \frac{p}{\rho u_0^2}$,
$Re = \frac{u_0 H}{\nu}$, $Gr = \frac{g\beta(T_h-T_c)H^3}{\nu^2}$, $Ri = \frac{g\beta(T_h-T_c)H}{u_0^2}$, $Pr = \frac{\nu}{\alpha}$.

Under the above circumstances, the governing system in nondimensional form can be expressed as

$$\frac{\partial U}{\partial X} + \frac{\partial V}{\partial Y} = 0, \tag{3.5}$$

$$U\frac{\partial U}{\partial X} + V\frac{\partial U}{\partial Y} = -\frac{\partial P}{\partial X} + \frac{1}{Re}\left(\frac{\partial^2 U}{\partial X^2} + \frac{\partial^2 U}{\partial Y^2}\right), \tag{3.6}$$

$$U\frac{\partial V}{\partial X} + V\frac{\partial V}{\partial Y} = -\frac{\partial P}{\partial Y} + \frac{1}{Re}\left(\frac{\partial^2 V}{\partial X^2} + \frac{\partial^2 V}{\partial Y^2}\right) + \frac{Gr}{Re^2}\theta, \tag{3.7}$$

$$U\frac{\partial \theta}{\partial X} + V\frac{\partial \theta}{\partial Y} = \frac{1}{PrRe}\left(\frac{\partial^2 \theta}{\partial X^2} + \frac{\partial^2 \theta}{\partial Y^2}\right). \tag{3.8}$$

The boundary conditions for the cavity walls in dimensionless form are reduced as follows:

$U = V = 0, \quad \theta = 1, \quad \text{at} \quad Y = 0, \qquad 0 \le X \le 1,$

$U = 1, \quad V = 0, \quad \theta = 0, \quad \text{at } Y = 1, \quad 0 \le X \le 1,$

$U = V = 0, \quad \frac{\partial \theta}{\partial X}=0, \quad \text{at } X = 0,\ 1, \quad 0 \le Y \le 1$

and the boundary conditions for circular cylinder are $U = V = 0$ for the velocity. Two types of thermal conditions have been considered and analyzed on surface of the cylinder. That is,

(a) For adiabatic : $\frac{\partial \theta}{\partial \mathbf{n}} = 0$

(b) For isothermal : $\theta = 0$,

where $\mathbf{n}$ is the unit normal vector to the boundary of the circular body.

3.2 Nusselt Number [26]

The local and average Nusselt numbers along the lower heated wall is determined by considering Tc as a reference temperature

$$Nu_Y = -\left(\frac{\partial \theta}{\partial Y}\right)_{Y=0},$$

the average Nusselt number Nu_{avg} is computed as

$$Nu_{avg} = \int_0^1 Nu_Y dX.$$

3.3 Solution Methodology

The governing equations (3.5) to (3.8) for the proposed problem together with defined boundary conditions are solved with the help of FEM based on Galerkin method. The solution details are mentioned as follows.

3.3.1 Weak Formulation

To obtain the variational or weak form, multiply the continuity equation by $\tilde{q} \in Q$, momentum and energy equations by $\tilde{w} \in \mathbf{W}$ where $Q = L^2(\Omega)$ and $\mathbf{W} = [H_1(\Omega)]^3$ and then integrate over the whole computational domain (Ω). Then, the weak form reads the following.

Find U, V and $\theta \in \mathbf{W}$ and $p \in$ Q such that

$$\begin{aligned}\int_\Omega \left(V\frac{\partial U}{\partial Y} + U\frac{\partial U}{\partial X}\right)\tilde{w}d\Omega + \int_\Omega \left(\frac{\partial P}{\partial X}\right)\tilde{w}d\Omega \\ - \triangle_1 \int_\Omega \left(\frac{\partial^2 U}{\partial Y^2} + \frac{\partial^2 U}{\partial X^2}\right)\tilde{w}d\Omega = 0,\end{aligned} \tag{3.9}$$

$$\begin{aligned}\int_\Omega \left(V\frac{\partial V}{\partial Y} + U\frac{\partial V}{\partial X}\right)\tilde{w}d\Omega + \int_\Omega \left(\frac{\partial P}{\partial Y}\right)\tilde{w}d\Omega \\ - \triangle_1 \int_\Omega \left(\frac{\partial^2 V}{\partial X^2} + \frac{\partial^2 V}{\partial Y^2}\right)\tilde{w}d\Omega - \triangle_2 \int_\Omega (\theta)\tilde{w}d\Omega = 0,\end{aligned} \tag{3.10}$$

$$\int_\Omega \left(\frac{\partial U}{\partial X}\right) \tilde{q} d\Omega + \int_\Omega \left(\frac{\partial V}{\partial Y}\right) \tilde{q} d\Omega = 0, \tag{3.11}$$

$$\int_\Omega \left(V\frac{\partial \theta}{\partial Y} + U\frac{\partial \theta}{\partial X}\right) \tilde{w} d\Omega + \triangle_3 \left(\int_\Omega \frac{\partial^2 \theta}{\partial Y^2} + \frac{\partial^2 \theta}{\partial X^2}\right) \tilde{w} d\Omega = 0, \tag{3.12}$$

where $\triangle_1 = \frac{1}{Re}$, $\triangle_2 = \frac{Gr}{Re^2}$, $\triangle_3 = \frac{\bigtriangledown^2}{PrRe}$, for all $\tilde{w}$ and $\tilde{q} \in \mathbf{W}$ and Q, respectively. Instead of dealing with infinite dimensional test and trial space we approximate these with finite dimensional test space $\mathbf{W_h} \approx \mathbf{W}$ and trial space $Q_h \approx Q$. That is $\tilde{w}_h \in \mathbf{W} \approx \mathbf{W_h}$ and $\tilde{q}_h \in Q \approx Q_h$, by implementing Green's theorem to reduce the order of derivatives of trial space we get at discrete level

$$\begin{aligned} \triangle_1 \int_\Omega \left(\frac{\partial U_h}{\partial X}\frac{\partial \tilde{w}_h}{\partial X} + \frac{\partial U_h}{\partial Y}\frac{\partial \tilde{w}_h}{\partial Y}\right) d\Omega + \int_\Omega \left(U_h\frac{\partial U_h}{\partial X} + V_h\frac{\partial U_h}{\partial Y}\right) \tilde{w}_h d\Omega \\ - \int_\Omega \left(\frac{\partial \tilde{w}_h}{\partial X}\right) P_h d\Omega = 0, \end{aligned} \tag{3.13}$$

$$\begin{aligned} \triangle_1 \int_\Omega \left(\frac{\partial V_h}{\partial X}\frac{\partial \tilde{w}_h}{\partial X} + \frac{\partial V_h}{\partial Y}\frac{\partial \tilde{w}_h}{\partial Y}\right) d\Omega + \int_\Omega \left(U_h\frac{\partial V_h}{\partial X} + V_h\frac{\partial V_h}{\partial Y}\right) \tilde{w}_h d\Omega \\ - \int_\Omega \left(\frac{\partial \tilde{w}_h}{\partial Y}\right) P_h d\Omega - \triangle_2 \int_\Omega (\theta_h)\tilde{w}_h d\Omega = 0, \end{aligned} \tag{3.14}$$

$$\int_\Omega \left(\frac{\partial U_h}{\partial X}\right) \tilde{q}_h d\Omega + \int_\Omega \left(\frac{\partial V_h}{\partial Y}\right) \tilde{q}_h d\Omega = 0, \tag{3.15}$$

$$\int_\Omega \left(U_h\frac{\partial \theta_h}{\partial X} + V_h\frac{\partial \theta_h}{\partial Y}\right) \tilde{w}_h d\Omega - \triangle_3 \int_\Omega (\theta_h)\tilde{w}_h d\Omega = 0, \tag{3.16}$$

where,

$U_h = \sum_{j=1}^{n} U_j \xi_j$, $V_h = \sum_{j=1}^{n} V_j \xi_j$, $\theta_h = \sum_{j=1}^{n} \theta_j \xi_j$ and $P_h = \sum_{j=1}^{m} P_j \psi_j$,

denotes the approximation of trail functions.

Similarly, the corresponding test functions can be expressed as:

$w_h = \sum_{i=1}^{n} \tilde{w}_i \xi_i$ and $\tilde{q}_h = \sum_{i=1}^{m} \tilde{q}_i \psi_i$.

By substituting these approximations in the above defined equations, the discretized system can be written in the matrix form as

$$\underbrace{\begin{bmatrix} K^{11} & K^{12} & K^{13} & K^{14} \\ K^{21} & K^{22} & K^{23} & K^{24} \\ K^{31} & K^{32} & K^{33} & K^{34} \\ K^{41} & K^{42} & K^{43} & K^{44} \end{bmatrix}}_{\mathbf{A}^\star} \underbrace{\begin{bmatrix} \underline{U} \\ \underline{V} \\ \underline{P} \\ \underline{\theta} \end{bmatrix}}_{\mathbf{U}^\star} = \underbrace{\begin{bmatrix} \underline{F_1} \\ \underline{F_2} \\ \underline{F_3} \\ \underline{F_4} \end{bmatrix}}_{\mathbf{F}^\star} \tag{3.17}$$

where $\mathbf{A}^\star$ is block matrix, $\mathbf{U}^\star$ is associated block vector and $\mathbf{F}^\star$ is associated block right hand side vector.

The entries of the corresponding local matrix can be written as:

$K_{ij}^{11} = \triangle_1 \int_\Omega \left(\frac{\partial \xi_j}{\partial X} \frac{\partial \xi_i}{\partial X} + \frac{\partial \xi_j}{\partial Y} \frac{\partial \xi_i}{\partial Y} \right) d\Omega + \int_\Omega \left(U \xi_j \frac{\partial \xi_i}{\partial X} \right) d\Omega + \int_\Omega \left(V \xi_j \frac{\partial \xi_i}{\partial Y} \right) d\Omega,$
$K_{ij}^{13} = \int_\Omega \left(\frac{\partial \xi_i}{\partial X} \psi_j \right) d\Omega,$
$K_{ij}^{21} = \triangle_1 \int_\Omega \left(\frac{\partial \xi_j}{\partial X} \frac{\partial \xi_i}{\partial X} + \frac{\partial \xi_j}{\partial Y} \frac{\partial \xi_i}{\partial Y} \right) d\Omega + \int_\Omega \left(U \xi_j \frac{\partial \xi_i}{\partial X} \right) d\Omega + \int_\Omega \left(V \xi_j \frac{\partial \xi_i}{\partial Y} \right) d\Omega,$
$K_{ij}^{23} = \int_\Omega \left(\frac{\partial \xi_i}{\partial Y} \right) \psi_j d\Omega, \qquad K_{ij}^{24} = \triangle_2 \int_\Omega (\xi_j) \xi_i d\Omega,$
$K_{ij}^{31} = \int_\Omega \left(\frac{\partial \xi_i}{\partial X} \right) \psi_j d\Omega, \qquad K_{ij}^{32} = \int_\Omega \left(\frac{\partial \xi_i}{\partial Y} \right) \psi_j d\Omega,$
$K_{ij}^{44} = \int_\Omega \left(U \frac{\partial \xi_i}{\partial X} \right) \xi_j d\Omega + \int_\Omega \left(V \frac{\partial \xi_i}{\partial Y} \right) \xi_j d\Omega - \triangle_3 \int_\Omega \left(\frac{\partial \xi_j}{\partial X} \frac{\partial \xi_i}{\partial X} + \frac{\partial \xi_j}{\partial Y} \frac{\partial \xi_i}{\partial Y} \right) d\Omega,$
and $K_{ij}^{12} = K_{ij}^{14} = K_{ij}^{22} = K_{ij}^{33} = 0.$

The velocity and temperature components are discretized using the biquadratic Q_2 element which is 3rd order accurate in the L_2 norm and 2nd order accurate in the H_1 norm. The pressure component is discretized using discontinuous P_1^{disc} having 2nd order and 1st order accuracy in the L_2 and H_1 norm respectively.
The non-linear discretized system of equations is linearized using Picard iteration method and then resulting linear system is solved utilizing Gaussian elimination method.

3.4 Code Validation and Grid Convergence

In order to validate the implemented finite element method, the average Nusselt number is compared using the obtained results from the present work and that of

Ref. [26] in the Table 3.1. The results obtained from the present code are in good agreement with previous results in the literature.

Ri	Isothermal cold cylinder			Adiabatic cylinder		
	Present study	Ref. [26][a]	Ref. [26][b]	Present study	Ref. [26][a]	Ref. [26][b]
0.01	2.939	2.92	2.91	2.284	2.24	2.21
1.00	3.510	3.50	3.47	3.388	3.33	3.32
5.00	4.701	4.69	4.67	4.083	4.06	4.06
10.00	5.038	5.04	4.99	4.469	4.50	4.40

Table 3.1: The comparison of Nu_{avg} at the lower hot surface of a square lid driven enclosure along with centrally located circular cylinder among Nek5000 CFD, Ref. [26] and with the present results. Moreover a and b represents the results obtained from Adina 8.8.3 CFD and Open source CFD solvers respectively.

3.5 Results and Discussion

Two dimensional, steady and incompressible combined convective flow and heat transport characteristics in a square cavity with circular body for different cases i.e., adiabatic, isothermal, with different Ri has been investigated, and application of FEM is used to solve the system of governing equations with the help of Galerkin method. Numerical results are compared in terms of plots, isotherms and streamlines.

The streamlines for different Ri in three different cases i.e., no cylinder, adiabatic and isothermal cylinders are analyzed in Figure 3.2 for the fixed $Pr = 0.7$, $Re = 100$ and $r_0/H = 0.2$. In forced convection case i.e., $Ri = 0.01$ in without cylinder case the flow circulates in the half upper region of cavity due to the upper moving wall. In mixed convection region i.e $Ri = 1$ and $Ri = 5$ the flow circulation can be noticed in whole the cavity i.e., the fluid velocity increases by increasing Ri in without cylinder case. For free convection case $Ri = 0.1$ the flow velocity for adiabatic cylinder case is higher than the other two cases i.e., without cylinder and isothermal cases. In mixed convection region i.e., by increasing Ri the streamlines are uniformly distributed around the circular body, and the flow circulation around the cylinder increases for both the cases i.e., adiabatic and isothermal cylinders. By comparing all three cases the flow velocity is lower in the isothermal case than other cases i.e., adiabatic and without cylinder with is due to thermal shielding effect which is because of isothermal cylinder. For different Ri the isotherms effected by cylinder for three different cases i.e., isothermal, adiabatic cylinders and no cylinder case are shown in Figure 3.3. Thermal shielding effect which is because of the isothermal cylinder is obvious in temperature profile shown in Figure 3.3. For forced convection case i.e., $Ri = 0.1$, the isotherms can be notice below the cylinder for isothermal case. Higher natural convection is noted by enhancing the value of Ri which leads to the greater uniformity of temperature in the cavity. In mixed convection regime the isotherms can be observe in whole the cavity in without and adiabatic cylinders cases i.e due to lower hot wall buoyancy effect shows its presence for both the cases discussed, but in the case of

isothermal cylinder all the streamlines are limited in the lower and left area of the cylinder in the cavity means that due to the effect of the isothermal cylinder the fluid is noted in low temperature in the right side of the cavity. Which is due to thermal shielding effect which is because of the isothermal cylinder.

The effect of different Ri, and cylinder on temperature profile is shown at different side of the cylinder in the cavity in Figures 3.4, 3.5 and 3.6. i.e., $Y = 0.15$ (below the circular cylinder), $X = .15$ (left side of the circular cylinder) and $X = 0.85$ (right side of the circular cylinder) respectively. Figure 3.4 for both (the isothermal cylinder and adiabatic cylinder) cases by increasing Ri temperature decreases everywhere in horizontal location. For each value of Ri temperature for isothermal case is lower than adiabatic case. Forced convection of heat transfer is dominant for both the cases i.e., isothermal and adiabatic. consequences of changing the Richardson numbers on temperature along adiabatic walls of the cavity can be seen in Figures 3.5 and 3.6 .i.e., $X = 0.15$ (for the left side of cylinder) and $X = 0.85$ (for right side of cylinder). The upper surface which moves from negative to positive x-axis direction indicates clock-wise flow effect, it leaves great impact on temperature gradient to the both left and right side of the circular body. As a consequence by changing the values of Ri and different boundary conditions enforced on cylinder, both effect the temperature gradient. In both Figures 3.5 and 3.6, force convection of heat transfer is dominant and for $X = 0.15$ and mixed convection heat transfer is dominant over free convection for $X = 0.85$. Moreover temperature for the isothermal case is lower than the adiabatic case due to thermal shielding effect which is because of isothermal cylinder.

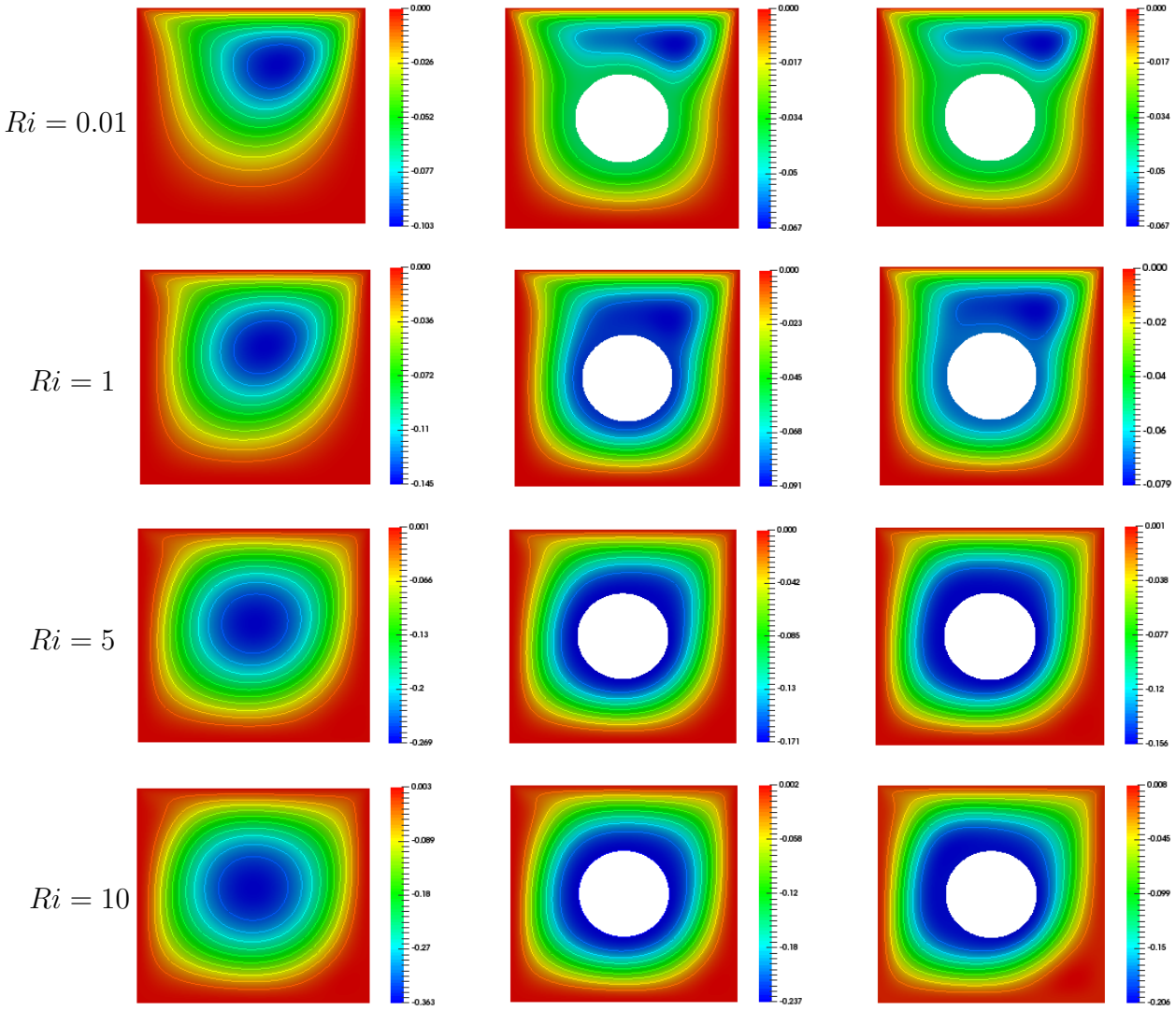

Figure 3.2: Streamlines for without Cylinder (Left), Adiabatic Cylinder (Center) and Isothermal Cylinder (Right) for Different Ri.

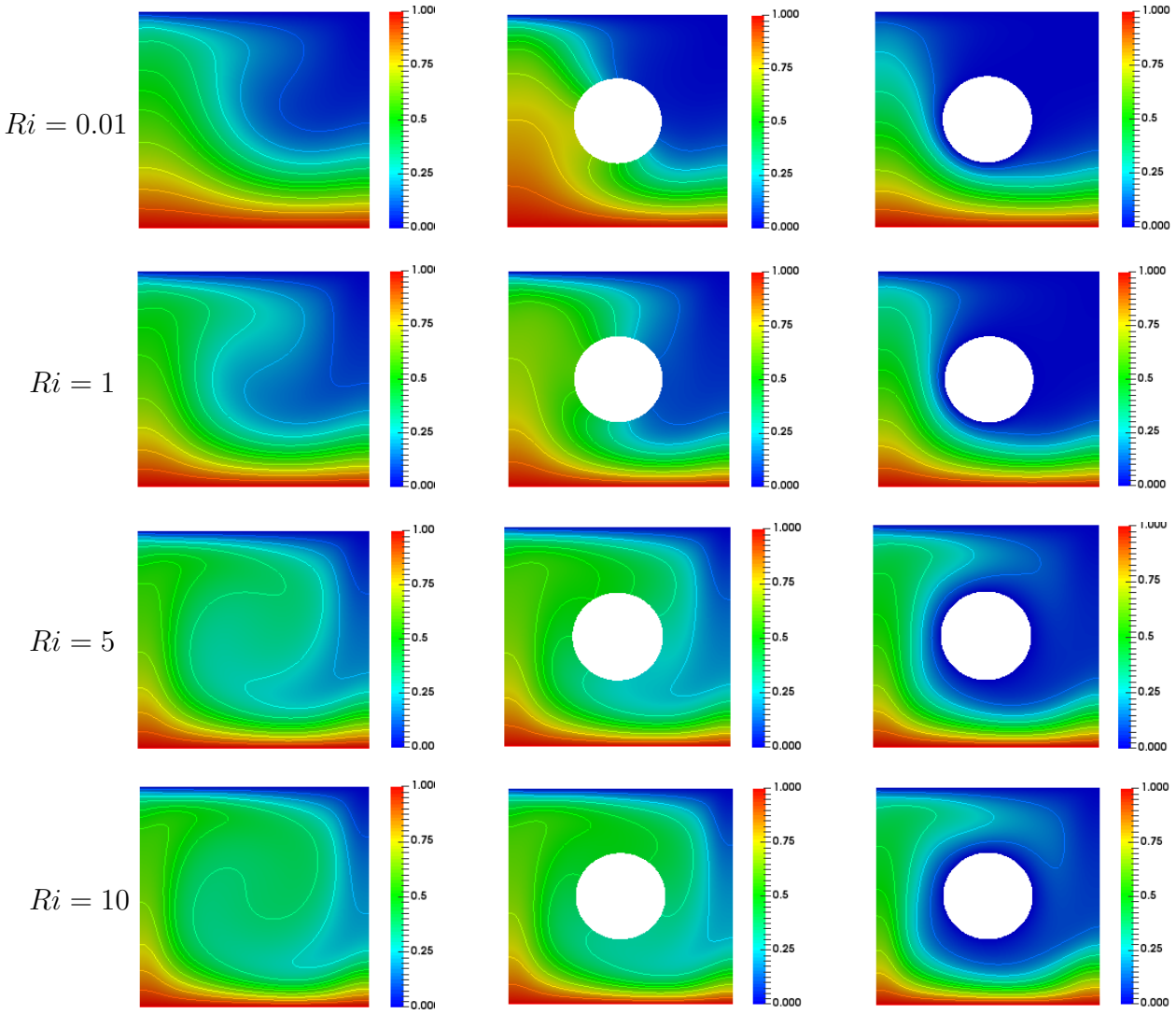

Figure 3.3: Isotherms for without Cylinder (Left), Adiabatic Cylinder (Center) and Isothermal Cylinder (Right) for Different Ri.

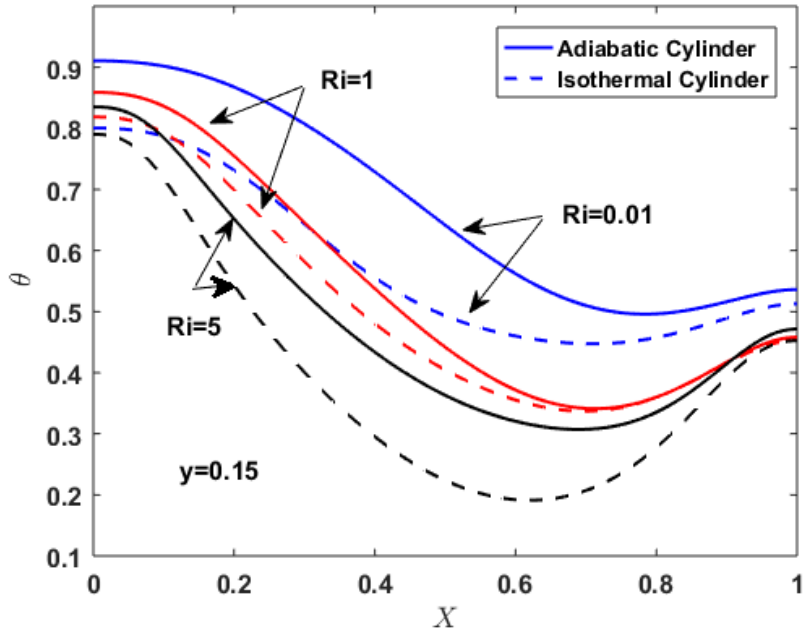

Figure 3.4: Impact of Different Ri on Temperature Profile along with Horizontal Plane for $Y = 0.15$ of Enclosure and $Re = 100$, $Pr = 0.7$, $r_0/H = 0.2$.

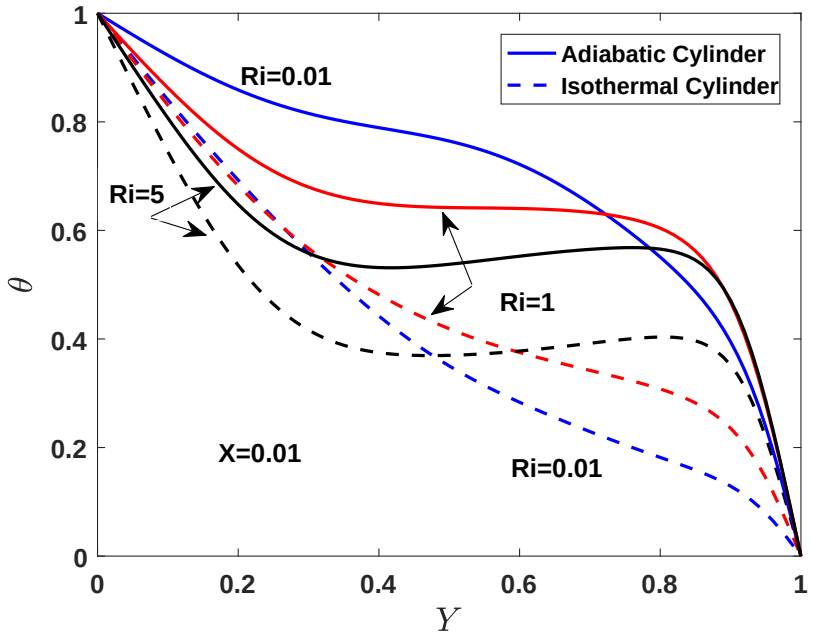

Figure 3.5: Impact of Different Ri on Temperature Profile along with Vertical Plane $X = 0.15$ of Enclosure $Re = 100$, $Pr = 0.7$, $r_0/H = 0.2$.

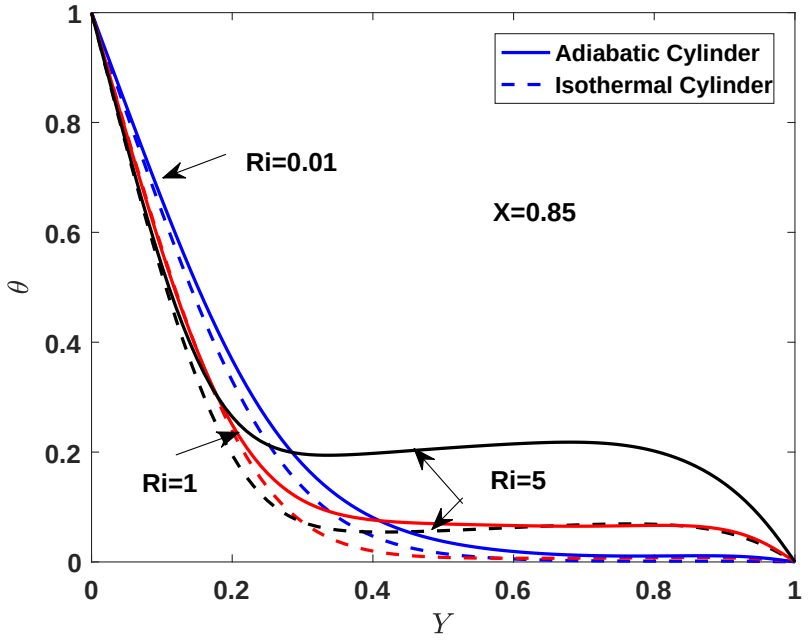

Figure 3.6: Impact of Different Ri on Temperature Profile along with Vertical Plane $X = 0.85$ of Enclosure $Re = 100$, $Pr = 0.7$, $r_0/H = 0.2$.

Chapter 4

MHD Combined Convection of Copper-Water Nanofluid in Lid Driven Enclosure with Circular Cylinder

In this chapter, the MHD combined convection of copper-water nanofluid flow in a square enclosure along with circular cylinder placed centrally in the cavity has been examined. The upper cold wall is moving with uniform speed, in the horizontal sides, vertical walls are taken adiabatic, and the lower wall is set at hotter temperature than upper wall. Numerical results have been analyzed in the form of tables, plots, streamlines, and isotherms. The work present in Chapter 3 is extended this chapter for the copper-water nanofluid.

4.1 Problem Formulation

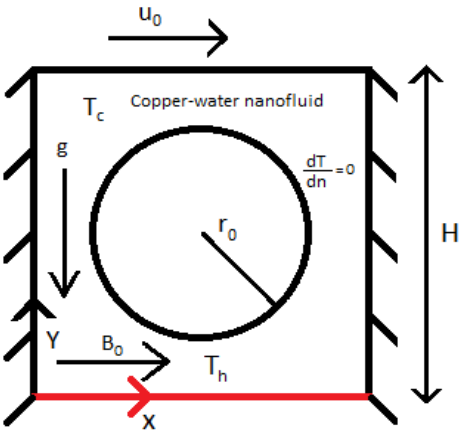

Figure 4.1: Schematic Diagram with Boundary Conditions and Coordinates.

Two dimensional, steady and incompressible MHD combined convection of copper-water nano-fluid flow and heat transport effect with circular body having radius $r_0/H = 0.2$ placed within the cavity of side length H is considered and analyzed. The upper horizontal surface is moving in the positive x-axis direction with fixed speed u_0. Vertical surfaces of the enclosure are taken as adiabatic. Cold temperature T_c and hot temperature T_h are enforced on the top moving and bottom walls, respectively, except $u = u_0$ at the top wall of the cavity no slip boundary conditions are applied on u and v velocities for each wall and cylinder in the cavity. Adiabatic boundary condition is imposed on the circular body. The magnetic field with strength B_0 is applied uniformly in x-direction. Moreover the induced magnetic field which is due to the motion of the fluid is neglected as compared with applying magnetic field. Moreover the Joule heating is considered and viscus dissipation, radiation, and slipping effects between two phases are neglected in the energy equation. The geometry of the proposed problem is presented in Figure 4.1.

Table 4.1: Thermo-Physical Characteristics of Base Fluid Water and Nanoparticle Copper

Property	$\rho(\mathrm{kg\,m^{-3}})$	$C_p(\mathrm{J\,kg^{-1}\,K^{-1}})$	$k(\mathrm{W\,m^{-1}\,k^{-1}})$	$\beta(\mathrm{K^{-1}})$
Water	997.1	4179	0.613	21×10^{-5}
Copper	8933	385	400	1.65×10^{-5}

The Governing Equations

Assuming the aforementioned situation, the two dimensional governing system of equations is

$$\frac{\partial u}{\partial x}+\frac{\partial v}{\partial y}=0, \tag{4.1}$$

$$u\frac{\partial u}{\partial x}+v\frac{\partial u}{\partial y}=-\frac{1}{\rho_{nf}}\frac{\partial p}{\partial x}+\frac{\mu_{nf}}{\rho_{nf}}\left(\frac{\partial^2 u}{\partial x^2}+\frac{\partial^2 u}{\partial y^2}\right), \tag{4.2}$$

$$u\frac{\partial v}{\partial x}+v\frac{\partial v}{\partial y}=-\frac{1}{\rho_{nf}}\frac{\partial p}{\partial y}+\frac{\mu_{nf}}{\rho_{nf}}\left(\frac{\partial^2 v}{\partial x^2}+\frac{\partial^2 v}{\partial y^2}\right)+\frac{(\rho\beta)_{nf}}{\rho_{nf}}g(T-T_c)-\frac{B_0^2\sigma_{nf}}{\rho_{nf}}v, \tag{4.3}$$

$$u\frac{\partial T}{\partial x}+v\frac{\partial T}{\partial y}=\alpha_{nf}\left(\frac{\partial^2 T}{\partial x^2}+\frac{\partial^2 T}{\partial y^2}\right)-\frac{B_0^2\sigma_{nf}}{(\rho C_p)_{nf}}v^2, \tag{4.4}$$

The Boundary Conditions

The subjected boundary conditions are as follows

$u=v=0, \quad T=T_h, \quad$ at $\quad y=0, \quad 0<x<1$

$u=u_0, \quad v=0, \quad T=T_c, \quad$ at $\quad y=1, \quad 0<x<1$

$u=0, \quad v=0, \quad \frac{\partial T}{\partial x}=0, \quad$ at $x=0,\,1, \quad 0\le y\le 1$

and for circular cylinder $\quad u=v=0, \quad \frac{\partial T}{\partial \mathbf{n}}=0.$

Thermo-Physical Properties [38]

Effective density, electrical conductivity, thermal diffusivity, coefficient of thermal expansion, and specific heat of the nano-fluid can be calculated by the following relations:

$$\rho_{nf}=\phi\rho_s+(1-\phi)\rho_f, \tag{4.5}$$

$$\sigma_{nf}=\sigma_f\left(\frac{3(\sigma-1)\phi}{(\sigma+2)-(\sigma-1)\phi}+1\right), \sigma=\frac{\sigma_s}{\sigma_f}, \tag{4.6}$$

$$\alpha_{nf}=\frac{k_{nf}}{(\rho C_p)_{nf}}, \tag{4.7}$$

$$(\rho\beta)_{nf}=\phi(\rho\beta)_s+(1-\phi)(\rho\beta)_f, \tag{4.8}$$

$$(\rho C_p)_{nf}=\phi(\rho C_p)_s+(1-\phi)(\rho C_p)_f, \tag{4.9}$$

where ϕ denotes the volume fraction for the nanofluid. Following is the estimated thermal conductivity of nanofluid using Maxwell model

$$\frac{k_{nf}}{k_f} = \frac{2k_f + k_s - 2\phi(k_f - k_s)}{2k_f + k_s + \phi(k_f - k_s)}, \tag{4.10}$$

where k_f and k_s are thermal conductivities of pure fluid and solid nanosized particles, respectively. Dynamic viscosity of nanofluid is given below using the Brinkman model

$$\mu_{nf} = \frac{\mu_f}{(1-\phi)^{2.5}}. \tag{4.11}$$

The Dimensionless Governing Equations

Using the following variables, the above defined governing equations into the dimensionless governing equations as follows

$X = \frac{x}{H}$, $Y = \frac{y}{H}$, $U = \frac{u}{u_0}$, $V = \frac{v}{u_0}$, $\theta = \frac{T-T_c}{T_h-T_c}$, $P = \frac{p}{\rho_{nf}u_0^2}$, $Re = \frac{u_0 H}{v_f}$, $Gr = \frac{g\beta(T_h-T_c)H^3}{\nu^2}$, $Ha = B_0 H\sqrt{\frac{\sigma_f}{\mu_f}}$, $P_r = \frac{\nu_f}{\alpha_f}$, $Ri = \frac{Gr}{Re^2}$, $Ec = \frac{u_0^2}{(C_p)_f(T_h-T_c)}$,

where ν_f, u_0, β and α_f are kinematic viscosity, imposed lid velocity, thermal expansion coefficient and the thermal diffusibility of nanofluid respectively and the gravitational acceleration is denoted by g. Using above dimensionless variables the dimensionless governing system of equations is

$$\frac{\partial U}{\partial X} + \frac{\partial V}{\partial Y} = 0, \tag{4.12}$$

$$U\frac{\partial U}{\partial X} + V\frac{\partial U}{\partial Y} = -\frac{\partial P}{\partial X} + \frac{1}{Re}\frac{1}{(1-\phi)^{2.5}}\frac{\rho_f}{\rho_{nf}}\left(\frac{\partial^2 U}{\partial X^2} + \frac{\partial^2 U}{\partial Y^2}\right), \tag{4.13}$$

$$\begin{aligned} U\frac{\partial V}{\partial X} + V\frac{\partial V}{\partial Y} = &-\frac{\partial P}{\partial Y} + \frac{1}{Re}\frac{1}{(1-\phi)^{2.5}}\frac{\rho_f}{\rho_{nf}}\left(\frac{\partial^2 V}{\partial X^2} + \frac{\partial^2 V}{\partial Y^2}\right) \\ &+Ri\frac{\rho_f}{\rho_{nf}}\left(1-\phi+\frac{\rho_s\beta_s}{\rho_f\beta_f}\phi\right)\theta - \frac{\rho_f}{\rho_{nf}}\frac{\sigma_{nf}}{\sigma_f}\frac{Ha^2}{Re}V, \end{aligned} \tag{4.14}$$

$$U\frac{\partial \theta}{\partial X} + V\frac{\partial \theta}{\partial Y} = \frac{\alpha_{nf}}{\alpha_f}\frac{1}{PrRe}\left(\frac{\partial^2 \theta}{\partial X^2} + \frac{\partial^2 \theta}{\partial Y^2}\right) + \frac{Ha^2 Ec}{Re}\frac{\sigma_{nf}}{\sigma_f}\frac{(\rho C_p)_f}{(\rho C_p)_{nf}}V^2. \tag{4.15}$$

The corresponding boundary conditions in nondimensional form are

$U = 0, \quad V = 0, \quad \theta = 1, \quad$ at $\quad Y = 0, \quad 0<X<1$

$U = 1, \quad V = 0, \quad \theta = 0, \quad$ at $\quad Y = 1, \quad 0<X<1$

$U = 0, \quad V = 0, \quad \frac{\partial\theta}{\partial X}=0, \quad$ at $\quad X = 0,1 \quad 0 \le Y \le 1$

and the boundary of circular cylinder is subjected to adiabatic thermal and no slip boundary conditions for velocity.
i.e., $U = V = 0$ and $\frac{\partial T}{\partial \mathbf{n}} = 0$

4.2 Physical Quantity of Interest [38]

The local Nu at the lower hot wall of the enclosure defined using below relations

$$Nu = \frac{h_{nf}}{T_h - T_c},$$

$$h_{nf} = \frac{q}{T_h - T_c},$$

$$q = -\frac{k_{nf}}{k_f}\frac{\partial \theta}{\partial Y},$$

where h_{nf} is coefficient of heat transfer, q is the wall heat flux. The local Nu at the lower hot wall of the enclosure defined as

$$Nu = -\frac{k_{nf}}{k_f}\left(\frac{\partial \theta}{\partial Y}\right)_{Y=0},$$

the average Nusselt number Nu_{avg} is computed as

$$Nu_{avg} = -\int_0^1 Nu dX.$$

4.3 Solution Methodology

The dimensionless system of governing equations (4.12) to (4.15) for the existing problem together with boundary conditions defined above are solved using FEM based on Galerkin method as in Chapter 3. Variational or weak form is obtained by multiplying each equation by their corresponding weight function and then integrated over the whole domain. Fixed point iteration method has been implemented

to linearize the non-linear system of discretized equations and the corresponding linearized system has been solved by Gaussian elimination technique.

4.3.1 Weak Formulation

To obtain the variational or weak form, multiply the continuity equation by $\tilde{q} \in Q$, momentum and energy equations by $\tilde{w} \in \mathbf{W}$ where $Q = L^2(\Omega)$ and $\mathbf{W} = [H_1(\Omega)]^3$ and then integrate over the whole computational domain (Ω). Then, the weak form reads the following.

Find U, V and $\theta \in \mathbf{W}$ and $p \in \mathrm{Q}$ such that

$$\begin{aligned}\int_\Omega \left(V\frac{\partial U}{\partial Y} + U\frac{\partial U}{\partial X}\right)\tilde{w}d\Omega + \int_\Omega \left(\frac{\partial P}{\partial X}\right)\tilde{w}d\Omega \\ - \triangle_1 \int_\Omega \left(\frac{\partial^2 U}{\partial Y^2} + \frac{\partial^2 U}{\partial X^2}\right)\tilde{w}d\Omega = 0,\end{aligned} \tag{4.16}$$

$$\begin{aligned}\int_\Omega \left(V\frac{\partial V}{\partial Y} + U\frac{\partial V}{\partial X}\right)\tilde{w}d\Omega + \int_\Omega \left(\frac{\partial P}{\partial Y}\right)\tilde{w}d\Omega + \triangle_3 \int_\Omega V\tilde{w}d\Omega \\ - \triangle_1 \int_\Omega \left(\frac{\partial^2 V}{\partial X^2} + \frac{\partial^2 V}{\partial Y^2}\right)\tilde{w}d\Omega - \triangle_2 \int_\Omega (\theta)\tilde{w}d\Omega - \triangle_2 \int_\Omega \theta\tilde{w}d\Omega = 0,\end{aligned} \tag{4.17}$$

$$\int_\Omega \left(\frac{\partial U}{\partial X}\right)\tilde{q}d\Omega + \int_\Omega \left(\frac{\partial V}{\partial Y}\right)\tilde{q}d\Omega = 0, \tag{4.18}$$

$$\int_\Omega \left(V\frac{\partial \theta}{\partial Y} + U\frac{\partial \theta}{\partial X}\right)\tilde{w}d\Omega + \triangle_4 \left(\int_\Omega \frac{\partial^2 \theta}{\partial Y^2} + \frac{\partial^2 \theta}{\partial X^2}\right)\tilde{w}d\Omega + \int_\Omega V^2\tilde{w}d\Omega = 0, \tag{4.19}$$

where $\triangle_1 = \frac{1}{Re}$, $\triangle_2 = \frac{Gr}{Re^2}$, $\triangle_3 = \frac{\nabla^2}{PrRe}$, for all $\tilde{w}$ and $\tilde{q} \in \mathbf{W}$ and Q, respectively. Instead of dealing with infinite dimensional test and trial space we approximate these with finite dimensional test space $\mathbf{W_h} \approx \mathbf{W}$ and trial space $Q_h \approx Q$. That is $\tilde{w}_h \in \mathbf{W} \approx \mathbf{W_h}$ and $\tilde{q}_h \in Q \approx Q_h$, by implementing Green's theorem to reduce the order of derivatives of trial space we get at discrete level

$$\begin{aligned}\triangle_1 \int_\Omega \left(\frac{\partial U_h}{\partial X}\frac{\partial \tilde{w}_h}{\partial X} + \frac{\partial U_h}{\partial Y}\frac{\partial \tilde{w}_h}{\partial Y}\right)d\Omega + \int_\Omega \left(V_h\frac{\partial U_h}{\partial Y} + U_h\frac{\partial U_h}{\partial X} + \right)\tilde{w}_h d\Omega \\ - \int_\Omega \left(\frac{\partial \tilde{w}_h}{\partial X}\right)P_h d\Omega = 0,\end{aligned} \tag{4.20}$$

$$\triangle_1 \int_\Omega \left(\frac{\partial V_h}{\partial X}\frac{\partial \tilde{w}_h}{\partial X} + \frac{\partial V_h}{\partial Y}\frac{\partial \tilde{w}_h}{\partial Y}\right) d\Omega + \int_\Omega \left(U_h \frac{\partial V_h}{\partial X} + V_h \frac{\partial V_h}{\partial Y}\right) \tilde{w}_h d\Omega - \int_\Omega \left(\frac{\partial \tilde{w}_h}{\partial Y}\right) P_h d\Omega - \triangle_2 \int_\Omega (\theta_h)\tilde{w}_h d\Omega + \triangle_3 \int_\Omega V \tilde{w}_h d\Omega = 0, \tag{4.21}$$

$$\int_\Omega \left(\frac{\partial U_h}{\partial X}\right) \tilde{q}_h d\Omega + \int_\Omega \left(\frac{\partial V_h}{\partial Y}\right) \tilde{q}_h d\Omega = 0, \tag{4.22}$$

$$\int_\Omega \left(U_h \frac{\partial \theta_h}{\partial X} + V_h \frac{\partial \theta_h}{\partial Y}\right) \tilde{w}_h d\Omega - \triangle_4 \int_\Omega \left(\frac{\partial \tilde{w}_h}{\partial X}\frac{\partial \theta}{\partial X} + \frac{\partial \tilde{w}_h}{\partial Y}\frac{\partial \theta}{\partial Y}\right) d\Omega + \triangle_5 \int_\Omega V^2 d\Omega = 0, \tag{4.23}$$

where,
$U_h = \sum_{j=1}^{n} U_j \xi_j$, $V_h = \sum_{j=1}^{n} V_j \xi_j$, $\theta_h = \sum_{j=1}^{n} \theta_j \xi_j$ and $P_h = \sum_{j=1}^{m} P_j \psi_j$,
denotes the approximation of trail functions.

Similarly, the corresponding test functions can be expressed as:
$w_h = \sum_{i=1}^{n} \tilde{w}_i \xi_i$ and $\tilde{q}_h = \sum_{i=1}^{m} \tilde{q}_i \psi_i$.
By substituting these approximations in the above defined equations, the discretized system can be written in the matrix form as

$$\underbrace{\begin{bmatrix} K^{11} & K^{12} & K^{13} & K^{14} \\ K^{21} & K^{22} & K^{23} & K^{24} \\ K^{31} & K^{32} & K^{33} & K^{34} \\ K^{41} & K^{42} & K^{43} & K^{44} \end{bmatrix}}_{\mathbf{A}^\star} \underbrace{\begin{bmatrix} \underline{U} \\ \underline{V} \\ \underline{P} \\ \underline{\theta} \end{bmatrix}}_{\mathbf{U}^\star} = \underbrace{\begin{bmatrix} \underline{F_1} \\ \underline{F_2} \\ \underline{F_3} \\ \underline{F_4} \end{bmatrix}}_{\mathbf{F}^\star} \tag{4.24}$$

where $\mathbf{A}^\star$ is block matrix, $\mathbf{U}^\star$ is associated block vector and $\mathbf{F}^\star$ is associated block right hand side vector.

The entries of the corresponding local matrix can be written as:
$K_{ij}^{11} = \triangle_1 \int_\Omega \left(\frac{\partial \xi_j}{\partial X}\frac{\partial \xi_i}{\partial X} + \frac{\partial \xi_j}{\partial Y}\frac{\partial \xi_i}{\partial Y}\right) d\Omega + \int_\Omega \left(U\xi_j \frac{\partial \xi_i}{\partial X}\right) d\Omega + \int_\Omega \left(V\xi_j \frac{\partial \xi_i}{\partial Y}\right) d\Omega,$
$K_{ij}^{13} = \int_\Omega \left(\frac{\partial \xi_i}{\partial X}\psi_j\right) d\Omega,$
$K_{ij}^{21} = \triangle_1 \int_\Omega \left(\frac{\partial \xi_j}{\partial X}\frac{\partial \xi_i}{\partial X} + \frac{\partial \xi_j}{\partial Y}\frac{\partial \xi_i}{\partial Y}\right) d\Omega + \int_\Omega \left(U\xi_j \frac{\partial \xi_i}{\partial X}\right) d\Omega + \int_\Omega \left(V\xi_j \frac{\partial \xi_i}{\partial Y}\right) + \xi_i \xi_j d\Omega,$
$K_{ij}^{23} = \int_\Omega \left(\frac{\partial \xi_i}{\partial Y}\right) \psi_j d\Omega,$ $K_{ij}^{24} = \triangle_2 \int_\Omega (\xi_j)\xi_i d\Omega,$
$K_{ij}^{31} = \int_\Omega \left(\frac{\partial \xi_i}{\partial X}\right) \psi_j d\Omega,$ $K_{ij}^{32} = \int_\Omega \left(\frac{\partial \xi_i}{\partial Y}\right) \psi_j d\Omega,$
$K_{ij}^{42} = \int_\Omega V^2 d\Omega$
$K_{ij}^{44} = \int_\Omega \left(U\frac{\partial \xi_i}{\partial X}\right) \xi_j d\Omega + \int_\Omega \left(V\frac{\partial \xi_i}{\partial Y}\right) \xi_j d\Omega + \triangle_4 \int_\Omega \left(\frac{\partial \xi_j}{\partial X}\frac{\partial \xi_i}{\partial X} + \frac{\partial \xi_j}{\partial Y}\frac{\partial \xi_i}{\partial Y}\right) d\Omega,$
and $K_{ij}^{12} = K_{ij}^{14} = K_{ij}^{22} = K_{ij}^{33} = 0,$

and

$\triangle_1 = \frac{1}{Re}\frac{1}{(1-\phi)^{2.5}}\frac{\rho_f}{\rho_{nf}}$,

$\triangle_2 = Ri\frac{\rho_f}{\rho_{nf}}\left(1-\phi+\frac{\rho_s\beta_s}{\rho_f\beta_f}\phi\right)$,

$\triangle_3 = \frac{\rho_f}{\rho_{nf}}\frac{\sigma_{nf}}{\sigma_f}\frac{Ha^2}{Re}$,

$\triangle_4 = \frac{\alpha_{nf}}{\alpha_f}\frac{1}{PrRe}$,

$\triangle_5 = \frac{Ha^2Ec}{Re}\frac{\sigma_{nf}}{\sigma_f}\frac{(\rho C_p)_f}{(\rho C_p)_{nf}}$.

The velocity and temperature components are discretized using the biquadratic Q_2 element which is 3rd order accurate in the L_2 norm and 2nd order accurate in the H_1 norm. The pressure component is discretized using discontinuous P_1^{disc} having 2nd order and 1st order accuracy in the L_2 and H_1 norm respectively. The non-linear discretized system of equations is linearized using Picard iteration method and then resulting linear system is solved utilizing Gaussian elimination method.

4.4 Results and Discussion

In this section, the impact of distinct parameters on MHD combined convection of coppe-water nanofluid in a lid driven square enclosure with circular cylinder placed inside has been analyzed. The standard values of the governing parameters are $Ha = 50$, $Ri = 10.0$, $\phi = 0.2$, $Re = 100$, and $Ec = 0.0001$ unless they are mentioned.

Figure 4.2 demonstrates the effect of different values of Eckert number (Ec) on streamlines and temperature. For increasing the values of Ec clearly shows the circulation of the streamlines around the circular body in the square cavity. By increasing the viscous dissipation upto $Ec = 0.005$ all the streamlines are shifted to upper region near moving wall in the cavity. Similarly isotherms for different values of Ec move diagonally from right bottom wall to left upper wall and it can be noted that by increasing viscous dissipation isotherms move towards upper moving wall. By increasing Eckert number upto $Ec = 0.005$ the isotherms distributed in the whole cavity. By increasing viscus dissipation the internal energy

of fluid increases due to which the temperature increases.

Figure 4.3 shows the impact of different values of Ha on the streamlines and isotherms for free or natural convection case ($Ri = 10$) for $Re = 100$, $Ec = 0.0001$, and $\phi = 0.2$. Streamlines are circulating around the circular body in the case of without magnetic field strength $Ha = 0$ and a small vortex near the right bottom corner can be seen due to moment of upper wall and buoyancy force. By increasing the magnetic field strength, the flow circulation around the circular body is reduced due to the effect of Lorentz force. By increasing magnetic field upto $Ha = 75$ and $Ha = 100$ all the streamlines are bounded to the upper region near moving wall, which shows the decrease in the velocity of the fluid due to the presence of strong Lorentz force. For lower values of Ha i.e., $Ha = 0$ and $Ha = 25$ most of the isotherms clustered near hot bottom wall and the left adiabatic wall due to top moving wall and lower hot wall. By increasing the magnetic field strength up to $Ha = 100$ the temperature increases, due to the presence of the strong Lorentz force the resistance in the motion of fluid against magnetic strength increases as a result the heat generates, in consequence of that the temperature increases.

Figure 4.4 demonstrates the impact of different values of Ri on streamlines and isotherms for $Ec = 0.0001$, $Re = 100$, $Ha = 50$, and $\phi = 0.2$. For $Ri = 0.1$ and $Ri = 1$, due to dominant shear forces all the streamlines are restricted to the upper region near hot wall above the circular body in the enclosure. By increasing the Richardson number buoyancy force shows its presence and some of the streamlines are distributed around the cylinder in the cavity. For higher values of Ri, i.e., $Ri = 10$ and $Ri = 20$, the movement of fluid can be observed in the whole cavity due to natural convection. For the case of force convection ($Ri = 0.1$), and for $Ri = 1$ isotherms are almost parallel to the hot wall due to convective mode of heat transfer, or due to buoyancy force. By increasing Richardson number upto $Ri = 5$, $Ri = 10$, and $Ri = 20$ streamlines move diagonally from the bottom of the left to the top of the right walls of the cavity due to the contribution of shear and buoyancy forces. For higher vales of Ri natural convection is dominant and due to strong buoyancy effect isotherms move from bottom hot wall towards moving

upper wall in the left side of the cavity.

Figure 4.5 displays the effect of different values of nanoparticles volume fractions (ϕ) on streamlines and isotherms for $Ha = 50$, $Ec = 0.0001$, and in the case of natural convection $Ri = 10$. For base fluid $\phi = 0$ most of the streamlines circulates in upper region of the cavity above the cylinder. By adding nanoparticles to the base fluid i.e., for $\phi = 0.05$, due to different behavior of the nanofluid from the base fluid some of the streamlines have been noticed around the cylinder. Moreover by increasing the volume fraction of nanofluid upto 0.2 the fluid movement can be noticed around cylinder throughout the cavity. Since density and viscosity of nanofluid are relatively higher than the base fluid, and by increasing ϕ thermal conductivity of nanofluid increases as a result heat transfer increases.

Figure 4.6 illustrates the influence of average Nusselt number (Nu_{avg}) for different values of volume fraction (ϕ) and Re. By increasing the concentration of nanoparticles (ϕ) the viscosity of resulting fluid increases and due to the improved thermo-physical characteristics of nanofluid heat transfer increases. Moreover by increasing Re the inertial forces increases and the resistance in fluid motion against viscosity increases due to this great resistance in the fluid heat transfer increases.

Figure 4.7 illustrates the influence of average nusselt number (Nu_{avg}) for different values of magnetic field strength (Ha) and Ri. By increasing Ri the convection mode of heat transfer increases so Nu_{avg} increases, and by increasing the value of Ha the strong Lorentz force has been generated which causes the decrease in fluid velocity and convection mode of heat transfer decreases due to which Nu_{avg} decreases.

Figure 4.8 illustrates the variation of average nusselt number (Nu_{avg}) along with Eckert number (Ec) for various values of Ri. By increasing viscus dissipation Ec average Nusselt number decreases. In particular heat gradually transfers from hot to cold region, here heat strength of lower hot wall is higher than heat strength

due to dissipation, effect therefore decrease in Nu_{avg} can be noted by increasing Ec.

Figure 4.9 illustrates the variation of average temperature (θ_{avg}) along with Eckert number (Ec) for various values of Ri. Increase in Ec causes increase in θ_{avg}. This conformed that Ec represents the relation between enthalpy and the kinetic energy in the flow. Ec converted the kinetic energy into internal or heat energy, which causes increase in temperature in the cavity.

Figure 4.10 illustrates the influence of average temperature (θ_{avg}) for different values of magnetic field strength (Ha) and Ri. Average temperature θ_{avg} increases by increasing Ri due to increase in convection mode of heat transfer. By increasing Ha, the resistance in fluid motion against strong Lorentz force increases due to this resistance heat generates which causes increase in temperature. Moreover due to inverse relation between magnetic effect and viscosity by increasing Ha heat transfer rate increases and hence the temperature increases.

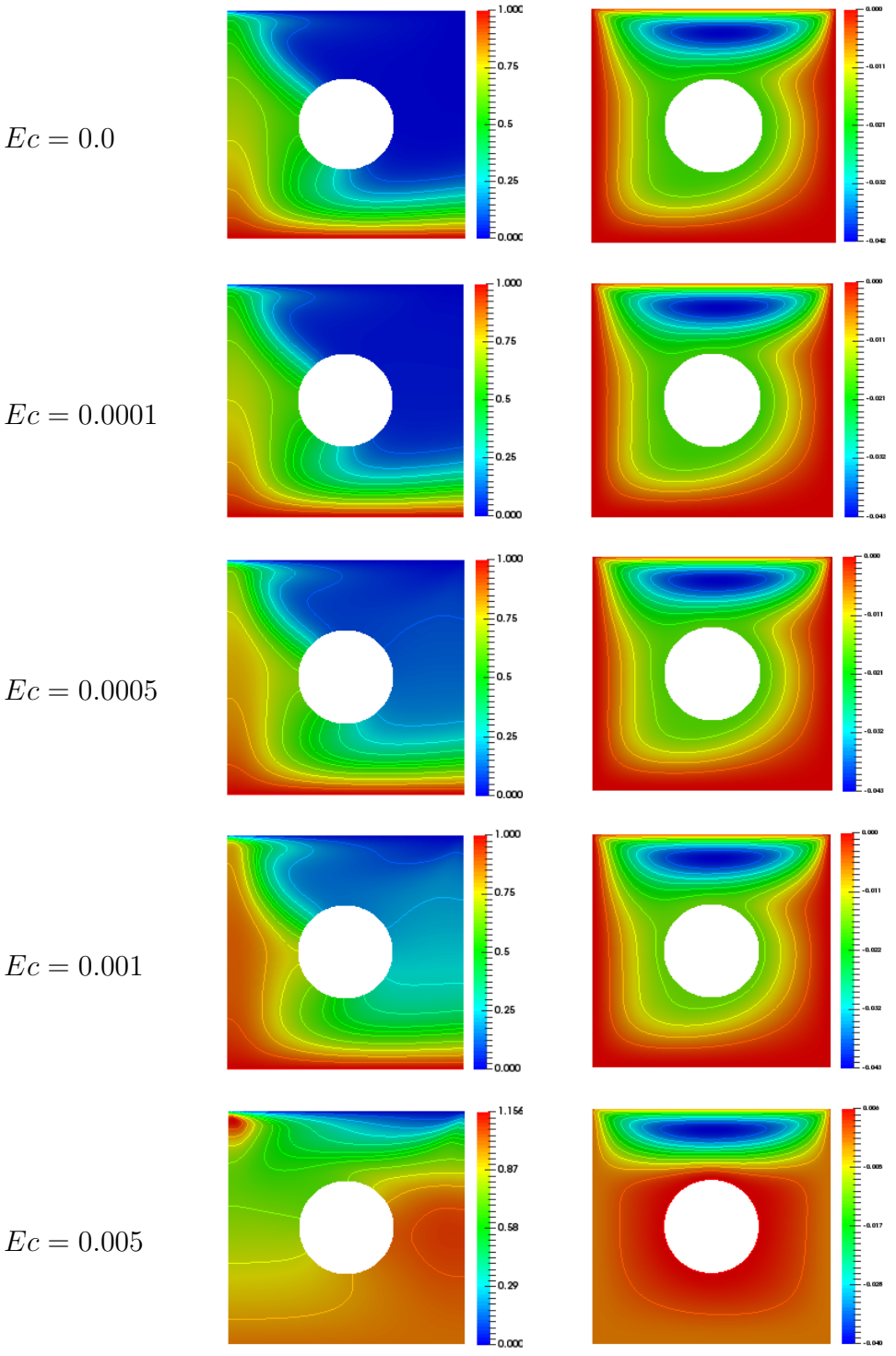

Figure 4.2: Variation of Isotherms (Left) and Streamlines (Right) for Distinct Ec with $Re = 100$, $\phi = 0.2$, $Ri = 10.0$, and $Ha = 50$.

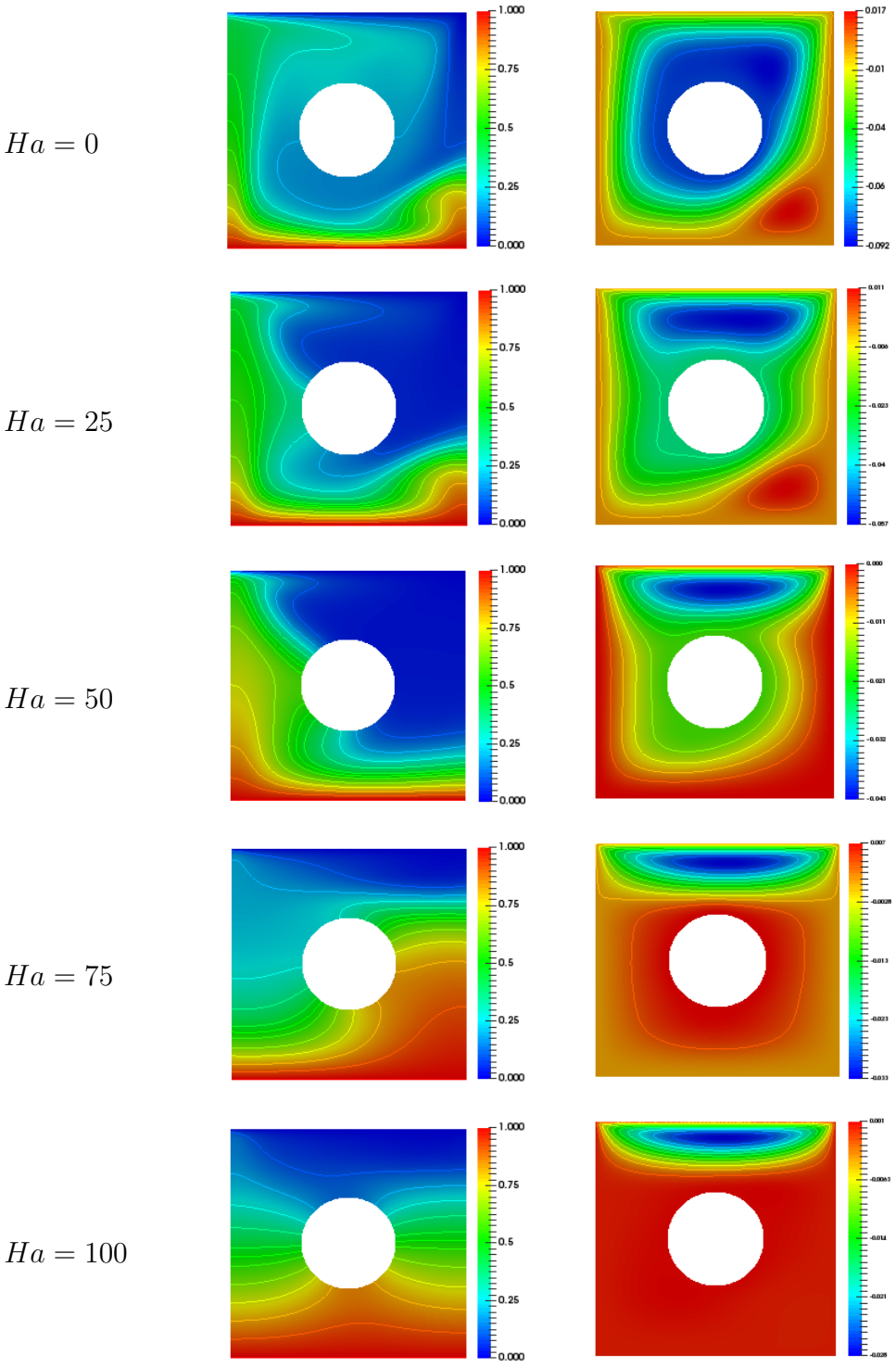

Figure 4.3: Variation of Isotherms (Left) and Streamlines (Right) with Distinct Values of Ha and for $Re = 100$, $Ec = 0.0001$, $Ri = 10.0$, and $\phi = 0.2$.

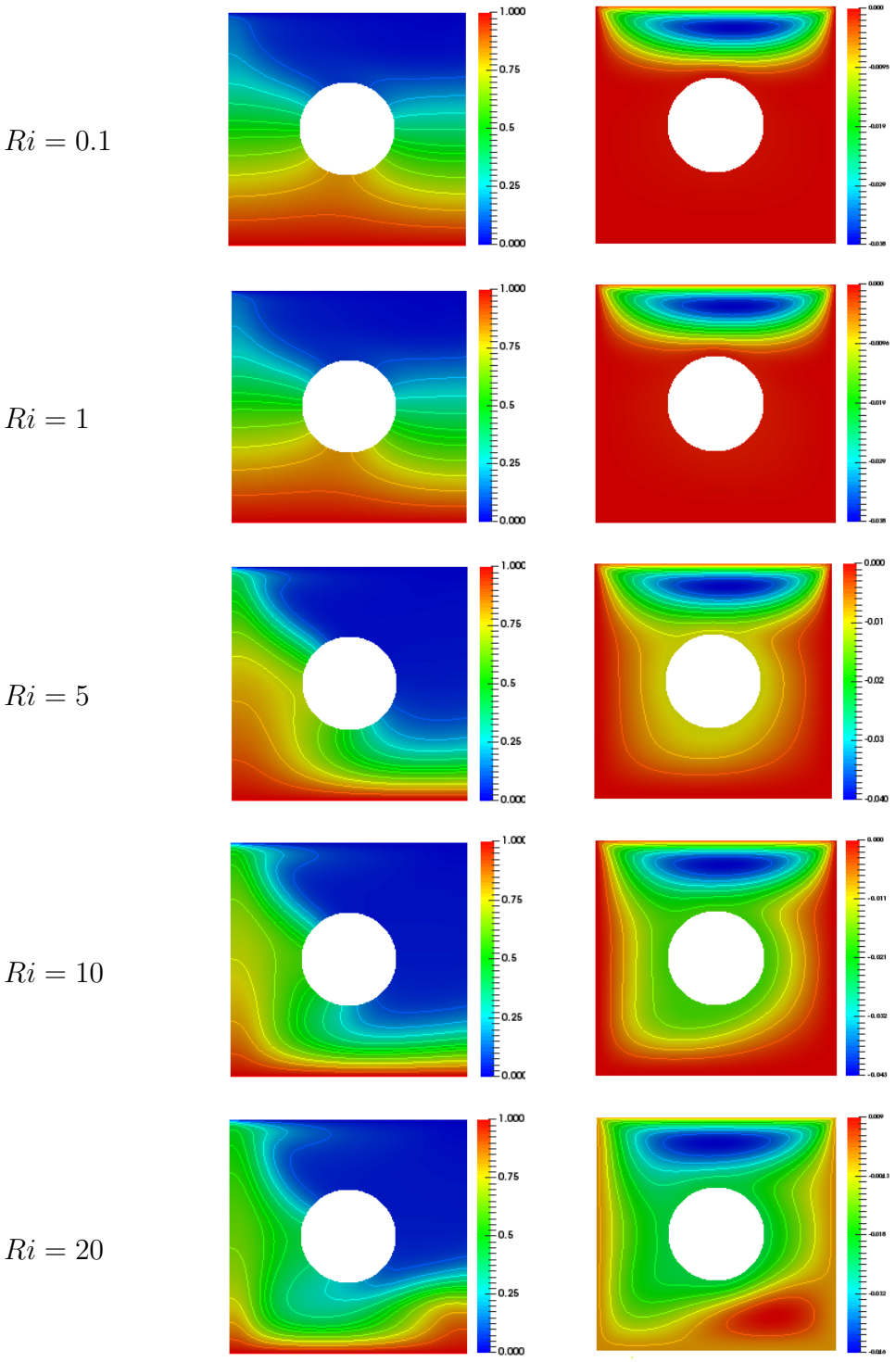

Figure 4.4: Variation of Isotherms (Left) and Streamlines (Right) with Distinct Values of Ri with $Re = 100$, $Ha = 50$, $\phi = 0.2$, and $Ec = 0.0001$.

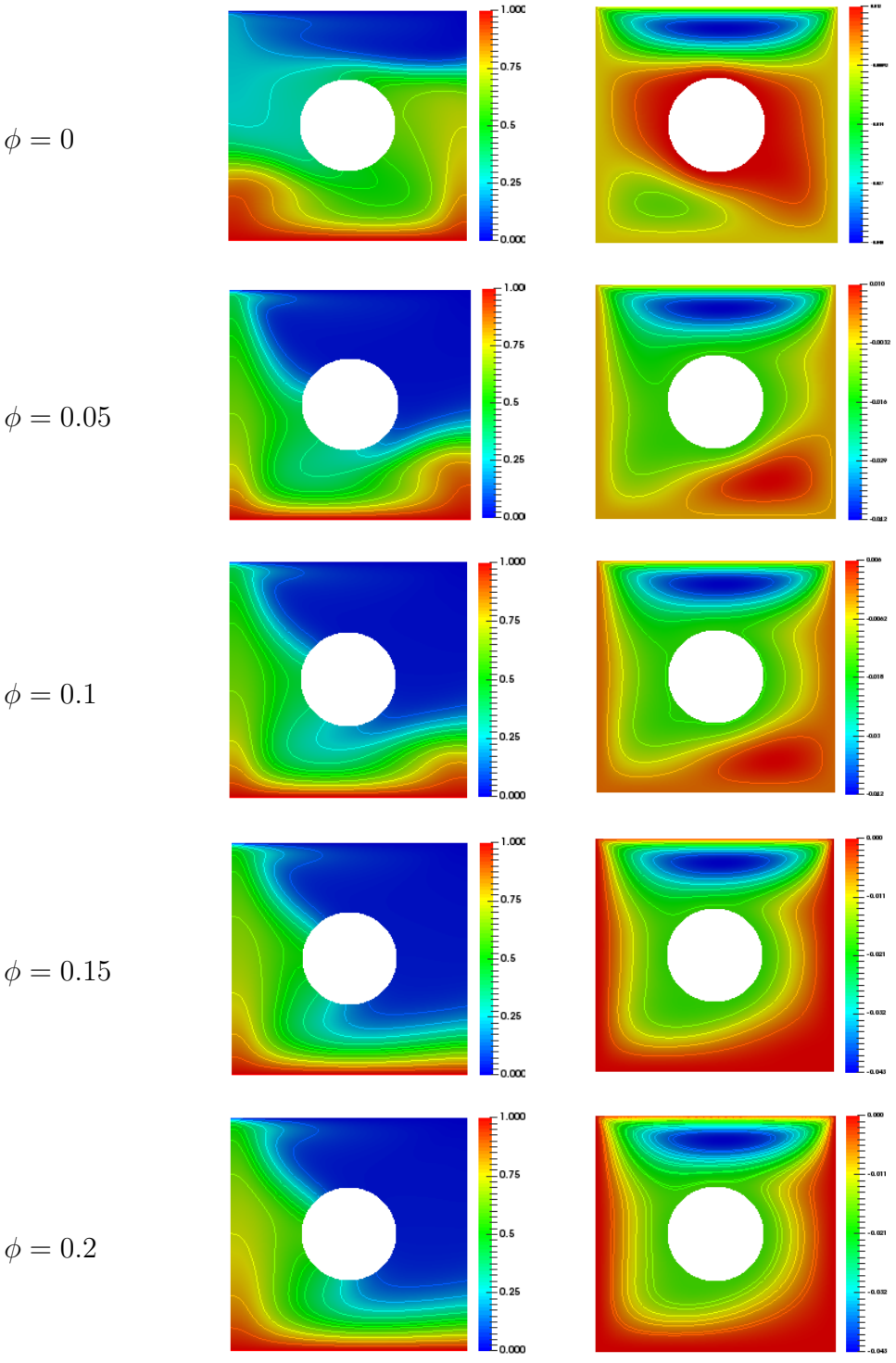

Figure 4.5: Variation of Isotherms (Left) and Streamlines (Right) with Distinct Values of ϕ with $Re = 100$, $Ri = 10.0$, $Ha = 50$, and $Ec = 0.0001$.

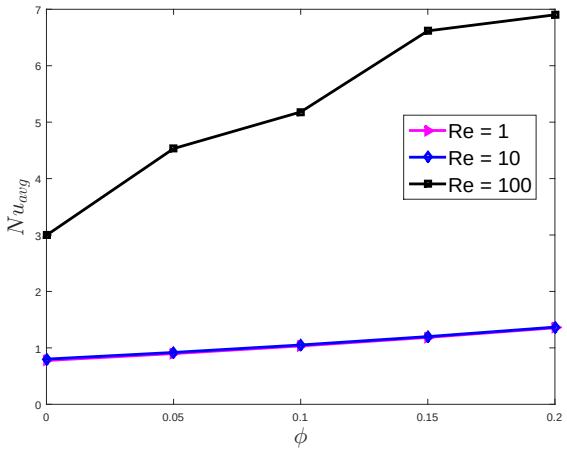

Figure 4.6: Variation of Nu_{avg} Along with ϕ for Different Re.

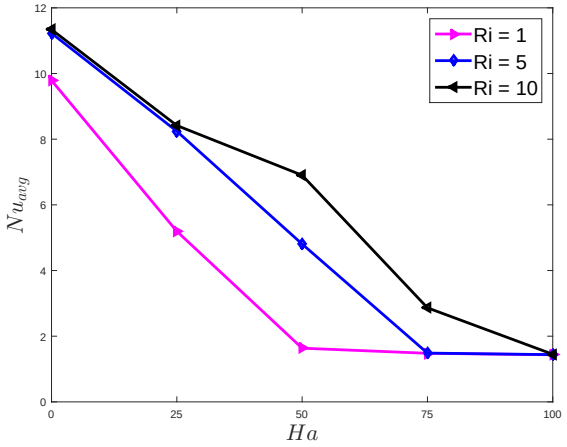

Figure 4.7: Variation of Nu_{avg} Along with Ha for Different Ri.

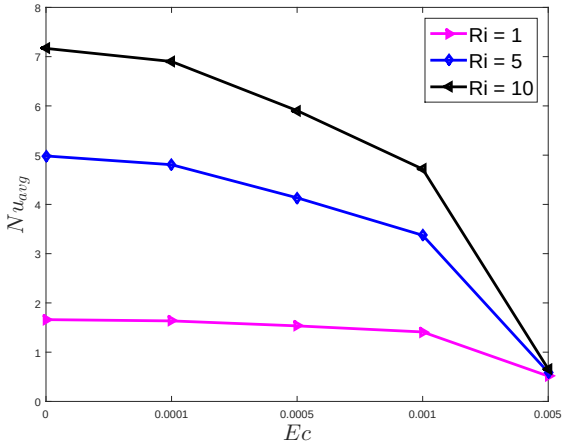

Figure 4.8: Variation of Nu_{avg} Along with Ec for Different Ri.

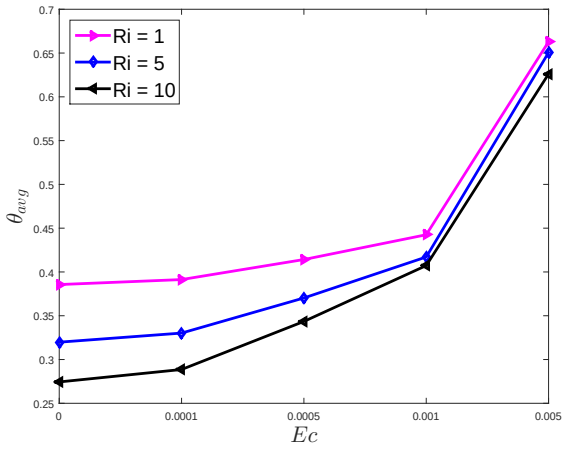

Figure 4.9: Variation of θ_{avg} as a Funtion of Ec for Different Ri.

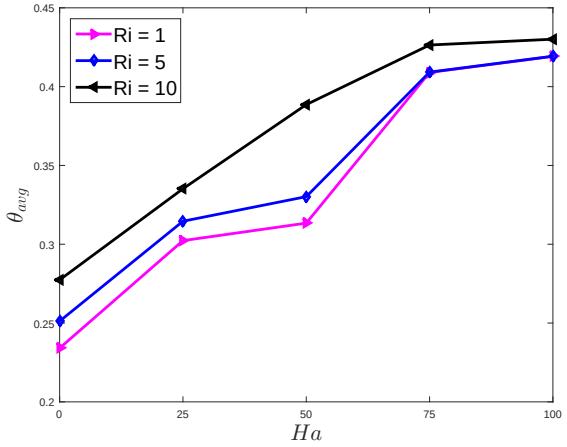

Figure 4.10: Variation of θ_{avg} as a Function of Ha for Different Ri.

Chapter 5

Conclusion and Outlook

In the present thesis, the analysis of steady two dimensional incompressible MHD combined convection of copper-water nanofluid in a lid driven cavity with circular cylinder has been performed. The vertical walls of the square cavity is considered adiabatic, upper wall and lower walls of the cavity are kept at cold and hot temperature respectively. Moreover no slip boundary conditions are applied on u and v velocities for each wall and cylinder in the cavity except the upper moving wall of the cavity where $u = u_0$ and $v = 0$. Furthermore, adiabatic circular cylinder is kept in the middle of the enclosure. First by taking appropriate transformations, the dimensional form of the governing equations are reduced into dimensionless form and then discretized using GFEM. The biquadratic Q_2 element is used to discretize the temperature and velocity components and for pressure component, the discontinuous linear P_1 element is used. Picard iterative method has been implemented to linearize the non-linear system of equations and the corresponding linearized system has been solved by Gaussian elimination technique. The impact of pertinent parameters on fluid flow, heat transfer and temperature distribution has been analyzed. The results have been analyzed in the forms of streamlines, isotherms and graphs. The present study leads to the following conclusions.

5.1 Conclusions

- By increasing the concentration of nanoparticles (ϕ) thermal conductivity increases as a result temperature in the cavity increases.
- By increasing nanoparticles volume fraction (ϕ) the thermal conductivity and viscosity of nanofluid increases as a consequence heat transfer increases.
- By increasing Re the inertial forces increases and the resistance in fluid flow against viscosity increases which causes increase in Nu_{avg}.
- By increasing magnetic field strength Ha due to strong Lorentz force the fluid velocity decreases.
- By increasing Ha velocity decreases and resistance of flow motion increases due to which average temperature increases.
- By increasing viscus dissipation (Ec) internal energy of fluid increases which causes increase in average temperature.

5.2 Future Recommendations

The present work can be extended in following directions.

- Circular heated cylinder or square body can be placed inside the cavity.
- Inclined cavity can be considered.
- The impact of porous media can be incorporated.
- Viscus dissipation can be assumed in the energy equation.

Bibliography

[1] B. Sreenivasulu, N. S. kirti, G. V. krishna, B R. Sree, and K. V. Ramesh. A numerical study on enhanced heat transfer in a lid driven cavity with and without fins. *International conference of Electronics, Communication and Aerospace Technology*, 2:611–616, 2017.

[2] S. B. Paramane and A. Sharma. Numerical investigation of heat and fluid flow across a rotating circular cylinder maintained at constant temperature in 2D laminar flow regime. *International Journal of Heat and Mass Transfer*, 52:3205 – 3216, 2009.

[3] S. Sivasankaran, H. T. Cheong, M. Bhuvaneswari, and P. Ganesan. Effect of moving wall direction on mixed convection in an inclined lid-driven square cavity with sinusoidal heating. *An International Journal of Computation and Methodology*, 69:630–642, 2016.

[4] R. Omari. Numerical investigation of a mixed convection flow in a lid driven cavity. *American Journal of computational Mathematics*, 6:251–258, 2016.

[5] N. B. Mansour, N. B. Cheikh, B. B. Beya, and T. Lili. Mixed convection of heat transfer in a square lid-driven cavity. *International Letters of Chemistry, Physics and Astronomy*, 55:180–186, 2015.

[6] T. Basak, S. Roy, P. K. Sharma, and I. Pop. Analysis of mixed convection flows within a square cavity with uniform and non-uniform heating of bottom wall. *International Journal of Thermal Sciences*, 48:891 – 912, 2009.

[7] O. A. Alawi, N. A. C. Sidik, and H. K. Dawood. Natural convection heat transfer in horizontal concentric annulus between outer cylinder and inner

flat tube using nanofluid. *International Journal of Heat and Mass Transfer*, 57:65 – 71, 2014.

[8] K. Khanafer and M. E. H. Assad. A numerical investigation of laminar mixed convection flow and heat transfer in a lid driven cavity with two cylinders. *Applied Mechanics and Materials*, 789-790:282–286, 2015.

[9] G. Cesini, M. Paroncini, G. Cortella, and M. Manzan. Natural convection from a horizontal cylinder in a rectangular cavity. *International Journal of Heat and Mass Transfer*, 42:1801 – 1811, 1999.

[10] K. Yahiaoui, D. Nehari, and D. Belkacem. The investigation of the mixed convection from a confined rotating circular cylinder. *Periodica Polytechnica Mechanical Engineering*, 61, 2017.

[11] V. A. F. Costa and A. M. Raimundo. Steady mixed convection in a differentially heated square enclosure with an active rotating circular cylinder. *International Journal of Heat and Mass Transfer*, 53:1208 – 1219, 2010.

[12] K. Khanafer and S. M. Aithal. Mixed convection heat transfer in a lid-driven cavity with a rotating circular cylinder. *International Communications in Heat and Mass Transfer*, 86:131 – 142, 2017.

[13] A. Raji and M. Hasnaoui. Mixed convection heat transfer in a rectangular cavity ventilated and heated from the side. *An International Journal of Computation and Methodology*, 33:533–548, 1998.

[14] S. F. Ferdousi, M. A. Alim, and R. Chowdhury. Prandtl number effect of mixed convection heat and mass transfer in a triangular enclosure with heated circular obstacle. *International Journal of Energy and Power Engineering*, 5: 39–47, 2016.

[15] S. Saha and M. Ali. Combined free and forced convection inside a two-dimensional multiple ventilated rectangular enclosure. *ARPN Journal of Engineering and Applied Sciences*, 1:23–35, 2006.

[16] R. Roslan, H. saleh, and I. Hashim. Natural convection in a differencially heated square enclosure with a solid polygon. *The Scientific World Journal*, 2014:1–11, 2014.

[17] M. M. Rehman, M. A. Alim, S. Saha, and M. K Chowdhury. Numerical study of mixed convection in a square cavity with a heat conducting sqaure cylinder at different location. *Journal of Mechanical Engineering*, 39:1–8, 2008.

[18] B. Ghasemi and S. M. Aminossadati. Numerical simulatoion of mixed convection in a rectangular enclosure with different numbers and arrangements of discrete heat sources. *The Arabian Journal for science and engineering*, 33:189–207, 2008.

[19] I. Khan, Shafquatullah, M. Y. Malik, A. Hussain, and M. Khan. Magnetohydrodynamics carreau nanofluid flow over an inclined convective heated stretching cylinder with joule heating. *Results in Physics*, 7:4001 – 4012, 2017.

[20] M. R. D. Garmroodi, A. Ahmadpour, and F. Talati. MHD mixed convection of nanofluids in the presence of multiple rotating cylinders in different configurations: A two-phase numerical study. *International Journal of Mechanical Sciences*, 150:247 – 264, 2019.

[21] K. H. Kabir, M. A. Alim, and L. S. Andallah. Effects of viscous dissipation on MHD natural convection flow along a vertical wavy surface with heat generation. *American Journal of Computational Mathematics*, 03:91–98, 2013.

[22] M. N. Uddin, M. A. Alim, and M. M. K. Chowdhury. Effects of mass transfer on MHD mixed convective flow along inclined porous plate. *Procedia Engineering*, 90:491 – 496, 2014.

[23] Fateh M. Oudina. Convective heat transfer of titania nanofluids of different base fluids in cylindrical annulus with discrete heat source. *Heat Transfer-Asian Research*, 48:135–147, 2019.

[24] A. Gul, I. Khan, and S. Shafie. Energy transfer in mixed convection MHD flow of nanofluid containing different shapes of nanoparticles in a channel

filled with saturated porous medium. *Nanoscale Research Letters*, 10:490, 2015.

[25] C. Veeresh, S. V. K. Varma, B. Rushi Kumar, and A.G. Vijaya Kumar. Heat and mass transfer in MHD mixed convection flow on a moving inclined porous plate. *International Journal of Engineering Research in Africa*, 20:144–160, 2016.

[26] K. Khanafer and S. M. Aithal. Laminar mixed convection flow and heat transfer characteristics in a lid driven cavity with a circular cylinder. *International Journal of Heat and Mass Transfer*, 66:200 – 209, 2013.

[27] R. W. Fox, A. T McDonald, and P. J. Pritchard. *Introduction to fluid mechanics sixth edition*. Wiley 6 edition, 2003.

[28] J. H. Ferziger and M. Peric. *Computational Methods for Fluid Dynamics*. Springer, 2002, 2002.

[29] R. K. Bansal. *A Textbook of Fluid Mechanics and Hydraulic Machines 9th Revised Edition SI Units (Chp.1-11)*. Laxmi Publications, 9th revised edition, 2010.

[30] K. S. Raju. *Fluid mechanics, heat Transfer, and mass transfer: chemical engineering practice*. Wiley-AIChE, 2011.

[31] F. M. White. *Fluid Mechanics 7th Edition*. McGraw-Hill Series in Mechanical Engineering. McGraw-Hill Education; 7 edition, 2010.

[32] R. W. Lewis, P. Nithiarasu, and K. N. Seetharamu. *Fundamentals of the finite element method for heat and fluid flow*. Wiley-AIChE, 2005, 2005.

[33] D. F. Young, B. R. Munson, T. H. okiishi, and W. W. Huebsch. *A brief introduction to fluid mechanics fifth edition*. Wiley-AIChE, 2010, 2010.

[34] Y. A. Cengel and J. M. Cimbala. *FLUID MECHANICS: FUNDAMENTALS AND APPLICATIONS*. McGraw-Hill, 1 edition, 2004.

[35] S. MOLOKOV, R. MOREAU, and H. K. MOFFATT. *Magnetohydrodynamics Historical Evolution and Trends*, volume 80. Springer, fourth edition, 2007.

[36] T. C. Papanastasiou, G. C. Georgios, and H. A. N. Alexandrou. *Viscous fluid flow*. CRC Press, 1999.

[37] J. Kunes. *Dimensionless physical quantities in science and engineering first edition*. Burlington, MA : Elsevier, 2012. - 658 p, 2012.

[38] K. Mehmood, S. Hussain, and M. Sagheer. Mixed convection in alumina-water nanofluid filled lid-driven square cavity with an isothermally heated square blockage inside with magnetic field effect. *International Journal of Heat and Mass Transfer*, 109:397–409, 2017.